Mathematical Biosciences 271 (2016) 1–18

Contents lists available at ScienceDirect

Mathematical Biosciences

journal homepage: www.elsevier.com/locate/mbs

Pattern formation – A missing link in the study of ecosystem response to environmental changes

Ehud Meron*

[a] Department of Solar Energy and Environmental Physics, Swiss Institute for Dryland Environmental and Energy Research, BIDR, Ben-Gurion University of the Negev, Sede Boqer Campus 8499000, Israel
[b] Department of Physics, Ben-Gurion University of the Negev, Beer Sheva, 8410501, Israel

ARTICLE INFO

Article history:
Received 28 May 2015
Revised 17 October 2015
Accepted 23 October 2015
Available online 31 October 2015

MSC:
35K55
35K57
45K05
92B05

PACS:
05.65.+b
87.23.Cc
89.75.−k

Keywords:
Vegetation pattern formation
Functional diversity
Desertification
Ecosystem engineers
Homoclinic snaking
Spatial resonances

ABSTRACT

Environmental changes can affect the functioning of an ecosystem directly, through the response of individual life forms, or indirectly, through interspecific interactions and community dynamics. The feasibility of a community-level response has motivated numerous studies aimed at understanding the mutual relationships between three elements of ecosystem dynamics: the abiotic environment, biodiversity and ecosystem function. Since ecosystems are inherently nonlinear and spatially extended, environmental changes can also induce pattern-forming instabilities that result in spatial self-organization of life forms and resources. This, in turn, can affect the relationships between these three elements, and make the response of ecosystems to environmental changes far more complex. Responses of this kind can be expected in dryland ecosystems, which show a variety of self-organizing vegetation patterns along the rainfall gradient. This paper describes the progress that has been made in understanding vegetation patterning in dryland ecosystems, and the roles it plays in ecosystem response to environmental variability. The progress has been achieved by modeling pattern-forming feedbacks at small spatial scales and up-scaling their effects to large scales through model studies. This approach sets the basis for integrating pattern formation theory into the study of ecosystem dynamics and addressing ecologically significant questions such as the dynamics of desertification, restoration of degraded landscapes, biodiversity changes along environmental gradients, and shrubland–grassland transitions.

1. Introduction

Much effort is devoted in ecology to the understanding of ecosystem response to environmental variability and to the impact of this response on ecosystem function [1–3]. A challenging question in this research effort is how do organism-level traits and small-scale spatial processes scale up to higher levels of organization and larger spatial scales, and determine ecosystem functions, such as bio-productivity and resilience in varying environments.

Species often develop organism-level mechanisms to cope with environmental stresses. These mechanisms generally involve phenotype changes [4], and are particularly relevant to immobile organisms, such as plants, which cannot migrate to less stressful environments. Plant species, for example, can maintain their water uptake under conditions of water stress by increasing the root-to-shoot ratio, or increase their specific leaf area in order to increase the interception of light in the shade. At higher organization levels and larger spatial scales additional mechanisms appear. Communities can respond to environmental stresses by changing their structure, and by self-organizing in spatial patterns.

A community-structure change is generally a combined result of environmental filtering and species interactions. Environmental filtering [5] is an organism-level process by which an initial community is selected out of a species pool in response to specific environmental conditions. The community is selected according to the distribution of response traits that determine the abilities of organisms to cope with environmental stresses. Interspecific interactions within the selected community induce community dynamics that further shape the community structure and determine the distribution of

* Correspondence address: Department of Physics, Ben-Gurion University of the Negev, Beer Sheva, 84105, Israel. Tel.: +972 8 6477556.
E-mail address: ehud@bgu.ac.il
URL: http://www.bgu.ac.il/~ehud

http://dx.doi.org/10.1016/j.mbs.2015.10.015
0025-5564/

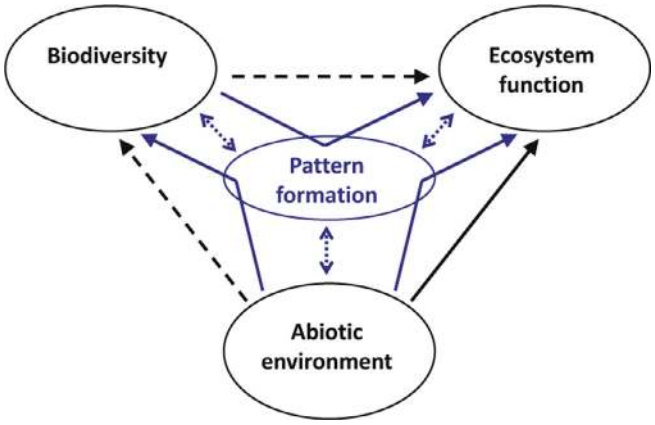

Fig. 1. The impact of environmental changes on ecosystem function. The abiotic environment can affect ecosystem function by its direct effect on any individual organism (solid black line), or indirectly by inducing a shift in community structure that changes the biodiversity of the system (two dashed black lines). Indirect relationships (broken solid blue arrows) can also be induced by pattern formation, which is linked to all three elements, the abiotic environment, biodiversity and ecosystem function (dotted blue arrows) (see the text for examples). Adapted from [12]. (For interpretation of the references to color in this figure legend, the reader is referred to the web version of this article).

effect traits – the traits that affect ecosystem function [6]. Scaling up organism-level attributes to community-level properties that determine ecosystem function involves then the identification of response and effect traits and the analysis of the complex nonlinear dynamics of large communities.

Spatial self-organization is induced by positive feedbacks that operate at small scales and lead to symmetry-breaking instabilities and pattern formation at large scales. An important context that shows such a response to environmental changes is water-limited vegetation [7–10]. Positive feedbacks in this context depend on organismic traits, such as biomass growth rate, water-uptake rate and root architecture, and on small-scale abiotic processes, such as overland water flow, surface-water infiltration and soil-water diffusion. Vegetation pattern formation is then a population-level response that increases water availability by the formation of vegetation patches and the transport of water toward the patch locations, a response that affects ecosystem functions such as resilience and bio-productivity. The spatial coupling and the resulting self-organized patchiness add another dimension to the complexity of the up-scaling problem.

The mediating role that community-level processes play in the response of ecosystems to environmental changes can be illustrated schematically by a diagram that relates three elements of ecosystem dynamics, as Fig. 1 shows [11]: the *abiotic environment*, representing rainfall, temperature, soil fertility, disturbances, etc., *biodiversity*, representing interspecific interactions, species richness, community composition, etc., and *ecosystem function*, which stands for biomass production, nutrient cycling, resilience, and other functions. The abiotic environment affects ecosystem function not only directly by the response of any organism as if other organisms were absent (solid black arrow), but also indirectly, through interspecific interactions that change community structure and the distribution of effect traits (dashed black arrows).

The main thesis we pursue here is that studies of ecosystem response to environmental changes should also scale up small-scale pattern-forming feedbacks, whenever they exist, and analyze the mediating effects of pattern formation. As Fig. 1 illustrates, pattern formation is directly linked to any of the three elements of ecosystem dynamics (small dotted blue arrows). It is linked to the abiotic environment because environmental stresses often induce spatially patterned states or transitions between different patterned states. It is linked to biodiversity because pattern formation generally involves resource redistribution, which affects interspecific interactions. It is also linked to ecosystem function since pattern formation involves changes in biomass production, resource-use efficiency, and ecosystem resilience. Understanding these and other links is essential for gaining a deeper insight into the processes that drive ecosystem dynamics and affect ecosystem function in varying environments.

We study these links using mathematical models of water-limited landscapes, employing the methods of pattern formation theory. Such landscapes provide a good case study in that they show a wide variety of vegetation patterns that are in good agreement with model predictions. The study of water-limited landscapes is significant also because it relates to two outstanding current problems in environmental research, desertification and biodiversity loss, and bears on the implications for ecosystem function.

We begin with a detailed description of the general mathematical model to be used and two simplified versions thereof that are motivated by specific ecological contexts (Section 2). We then briefly describe a few model studies of processes that link pattern formation to the abiotic environment, to biodiversity and to ecosystem function (Section 3), and discuss manners by which these processes can mediate the relationships between these three elements (Section 4). We conclude with a few remarks on the significance of pattern formation processes to other types of terrestrial ecosystems and to marine ecosystems, and on the reciprocal benefits of studying complex ecosystems to pattern formation theory (Section 5).

2. Modeling water-limited landscapes

Two main modeling approaches are in use in studies of plant population dynamics, agent-based models (also called individual-based models) [13], and partial differential equations (PDEs). The former are computational algorithms that go down to the level of individual plants and often describe them in great detail. The latter do not address individual plants but rather processes at small spatial scales, and characterize the population by a continuous biomass areal density. We use here the PDEs approach since it lends itself to the powerful methods of pattern formation theory [12,14,15].

2.1. Continuum modeling of discrete plant populations

The biomass of a plant population in a water limited system can often be regarded as a continuous deterministic variable for two main reasons [12]. The first is related to the modular design that dryland plants typically have. Rather than having a single stem that acts as an integrated hydraulic system, and is vulnerable to hydraulic failures caused by droughts, dryland plants often develop hydraulically independent multiple stems. The redundancy of independent conduits increases the plant's resistance to drought, as a failure of a single or a group of conduits can lead to partial plant mortality but still leaves the plant viable [16]. As a consequence, the response of a plant individual to water stress often involves a gradual biomass decrease rather than a sharp mortality event. The second reason is related to the availability of long-lived seeds and their non-vanishing probability to germinate whenever the biotic and abiotic conditions allow, which reduce strong population fluctuations and prevent the extinction of small populations. These considerations suggest the description of a plant population in terms of a deterministic continuous biomass variable, representing the above-ground biomass per unit area, irrespective of the number or identity of the plant individuals contributing to it.

Another question is how detailed continuum models should be [12]. Obviously, in order to account for vegetation pattern formation the models should capture pattern-forming feedbacks, i.e. feedbacks that can induce nonuniform instabilities of uniform vegetation. This has already been achieved with a single-variable model for the population biomass that does not take into account the associated

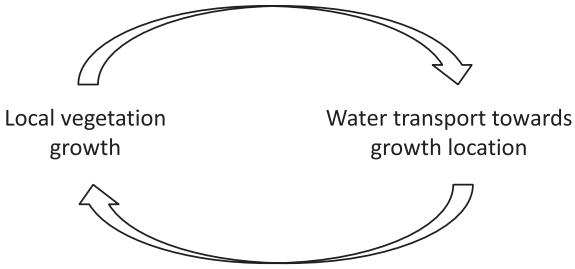

Fig. 2. Schematic illustration of the general positive feedback that drives vegetation pattern formation in water limited systems. While accelerating vegetation growth in existing patches these precesses inhibit the growth in the patch surroundings, thereby favoring vegetation pattern formation. From [12].

water dynamics [17]. More detailed models include an additional water variable [18–20], or two water variables representing soil-water content and overland water flow [21,22]. The more detailed models are advantageous for several reasons; they capture additional pattern-forming feedbacks, introduce better defined and measurable parameters, and provide a better account of the roles that various physical factors play in pattern-formation processes. On the other hand, detailed models are less amenable to mathematical analysis.

To benefit from both aspects we will consider a relatively detailed model for water-limited vegetation that captures three different pattern-forming feedbacks, but also study specific contexts that allow simplifications of the model by eliminating one or two feedbacks.

2.2. Three pattern forming feedbacks

The three pattern-forming feedbacks to be modeled can all be viewed as different realizations of a single general feedback. As Figs. 2 and 3 illustrate, this is a positive feedback between local vegetation growth and water transport towards the growing vegetation, where the three feedbacks differ in the mechanism of water transport - overland water flow, water conduction by laterally extended root systems, and soil-water diffusion, as explained in the following subsections. While the transport of water towards denser vegetation patches helps further vegetation growth there, it inhibits the growth in the vicinities of these patches and, thereby, favors nonuniform vegetation growth and pattern formation. On a slope or in the presence of wind, another pattern-forming feedback, associated with water advection, becomes feasible [18,23,24].

2.2.1. Infiltration feedback

Bare-soil areas in water-limited systems, i.e. areas devoid of vegetation, are often covered by thin biogenic soil crusts consisting of one or more organisms, such as cyanobacteria, green algae, fungi and lichens [25]. Soil crusts can induce overland water-flow by changing the rate of surface-water infiltration into bare soil. Crusts dominated by cyanobacteria, for example, can absorb water several times their dry weight in only a few seconds [26]. This results in crust swelling and soil-pore blocking and, consequently, in a significant reduction in water infiltration shortly after rain starts [27,28]. Since cyanobacteria are photosynthetic organisms, their growth is hindered by vegetation that blocks sunlight. As a consequence, the infiltration rates in sparsely vegetated or bare-soil areas are lower than those in densely vegetated areas[1]. This infiltration contrast induces overland water flow towards densely vegetated areas (see Fig. 3(a)), which accounts for the right arrow in Fig. 2, i.e. enhancement of water transport by local vegetation growth. The increased soil moisture in the growth location further increases the vegetation growth rate (left arrow in Fig. 2) and closes the positive feedback loop. We refer to this pattern-forming feedback as the *infiltration feedback*.

The infiltration feedback is modeled by assuming a monotonically increasing dependence of the infiltration rate I on the above-ground vegetation biomass B, which asymptotes to a constant maximal value A [21,22,32],

$$I = A\frac{B + Qf}{B + Q}, \tag{1}$$

where Q and $f \in [0, 1]$ are constants. The parameter f controls the infiltration contrast. When $f = 1$, $I = A$ is a constant independent of B. This limit represents no infiltration contrast between bare and vegetated soil areas and, therefore, no infiltration feedback. It may be approached in uncrusted sandy soils in which the infiltration rate is high everywhere and no overland water flow takes place. The other extreme, $f \ll 1$, represents a high infiltration contrast, $I = Af \ll A$ in bare soil and $I \to A$ in densely vegetated soil, and, therefore, strong infiltration feedback. The parameter Q measures how fast the infiltration rate reaches its maximal value A.

2.2.2. Root-augmentation feedback

The biomass of a plant consists of above-ground or shoot biomass and below-ground or root biomass. These two entities, however, are not independent; the relation between the two is expressed in terms of the root-to-shoot ratio, normally measured as the ratio of the root biomass to the shoot biomass. This ratio is monotonically increasing (the larger the shoot biomass the larger the root biomass), but generally not constant; variations in root-shoot biomass allocation can

[1] Additional factors contributing to this outcome include soil mounds generated by dust deposition that help the interception of runoff at vegetated patches [29], higher soil porosity in vegetation patches and others [30,31].

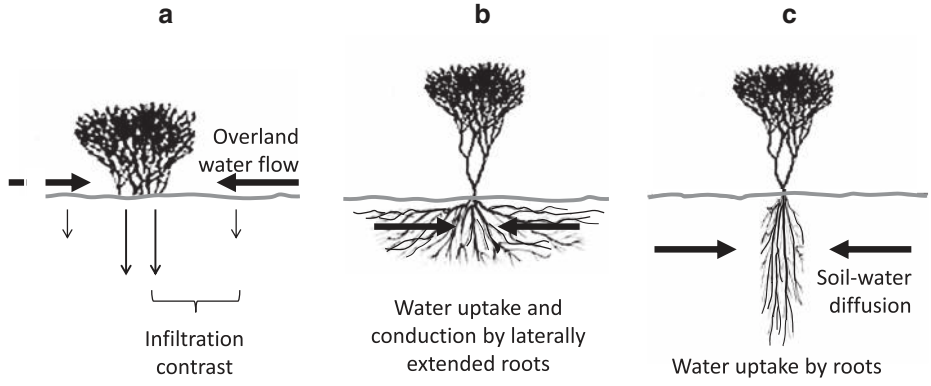

Fig. 3. Schematic illustrations of three modes of water transport capable of inducing pattern-forming feedbacks in water-limited vegetation: (a) overland water flow induced by an infiltration contrast (infiltration feedback), (b) water uptake and conduction by laterally extended root systems (root-augmentation feedback), (c) fast soil-water diffusion relative to biomass spread (soil-water diffusion feedback). From [12].

occur among individuals of the same species due to plasticity [33], and even during the growth of a single individual [34] due to ontogenetic drift [35]. From a modeling point of view we may choose the above-ground biomass, B, to be the independent variable, and express the root system in terms of B. The lateral extension of the root zone as the shoot grows is another mechanism by which vegetation growth enhances water transport, as the extended root zone allows water uptake and conduction from a larger domain (see Fig. 3(b)). This process and the consequent accelerated vegetation growth define the *root-augmentation feedback*.

The root-augmentation feedback is modeled by introducing a kernel function,

$$G(\mathbf{X},\mathbf{X}') = \tilde{G}\left(\frac{|\mathbf{X}-\mathbf{X}'|}{S[B(\mathbf{X})]}\right), \tag{2}$$

that describes the spatial distributions of the roots in the lateral directions X and Y. Here $\mathbf{X} = (X, Y)$ represents the plant (shoot) location and $\mathbf{X}'$ a distant point. The kernel function tails off to zero as $|\mathbf{X}-\mathbf{X}'|$ increases beyond a characteristic length, S, which represents the lateral extension of the root zone. The root-augmentation feedback is captured by letting S increase monotonically with the above-ground biomass $B(\mathbf{X})$. For simplicity we choose here a linear biomass dependence

$$S = S_0(1+EB), \tag{3}$$

where the constant parameter $E = S_0^{-1}dS/dB$ provides a measure for the root-to-shoot ratio and quantifies the strength of the root-augmentation feedback.

2.2.3. Soil-water diffusion feedback

A third mechanism of water transport towards a patch of growing vegetation is water depletion induced by local uptake, followed by soil-water diffusion from the patch surroundings (see Fig. 3(c)). The associated *soil-water diffusion feedback* also relies on the root-to-shoot property of plants, as the root-augmentation feedback does, except that the role of the roots is the creation of soil-water gradients due to local water uptake. This pattern-forming feedback may apply to plants with vertical roots and strong water uptake, and soil types that allow for fast lateral water diffusion relative to the rate of vegetation spread. Viewing the vegetation spread as a biomass diffusion process, the soil-water diffusion feedback can be associated with a Turing mechanism where pattern formation results from the time-scale disparity of different diffusive processes.

2.3. Model equations

We present here a mathematical model that was introduced by Gilad et al. [22,36] to describe vegetation patchiness formed by a single plant species in a water-limited system and later on has been extended to describe a plant community [37]. The models capture all three pattern-forming feedbacks, infiltration, root-augmentation and soil-water diffusion, but can be simplified, for specific ecological contexts, to capture only two or even a single feedback. In what follows we describe the models and their simplified forms and discuss non-dimensional forms thereof.

2.3.1. A single plant population

The Gilad et al. model contains three state variables: a biomass variable, $B(\mathbf{X}, T)$, representing the above-ground biomass per unit ground area, a soil-water variable, $W(\mathbf{X}, T)$, describing the soil-water content available to the plants per unit ground area, and a surface water variable, $H(\mathbf{X}, T)$, representing a thin water layer above ground level. Here $\mathbf{X} = (X, Y)$ represents the spatial coordinates and T the time coordinate (throughout this paper we use capital letters to denote dimensional quantities). The model equations are:

$$\partial_T B = G_B[B,W]B(1-B/K) - M(B)B + D_B\nabla^2 B, \tag{4a}$$

$$\partial_T W = I(B)H - L(B)W - G_W[B]W + D_W\nabla^2 W, \tag{4b}$$

$$\partial_T H = P - I(B)H - \nabla\cdot\mathbf{J}, \tag{4c}$$

where

$$\mathbf{J} = -2D_H H\nabla(H+Z), \tag{5}$$

$\nabla = \hat{\mathbf{x}}\partial_X + \hat{\mathbf{y}}\partial_Y$ ($\hat{\mathbf{x}}$ and $\hat{\mathbf{y}}$ being unit vectors in the x and y directions), and G_B, I, L and G_W are either functions (round brackets) or functionals (square brackets] of the denoted state variables to be described below. Temporal biomass changes are affected by water dependent plant growth $G_B B$, by mortality $-MB$, and by short-distance seed dispersal or clonal vegetation expansion from nearby plants $D_B\nabla^2 B$. The late biomass growth phase is also affected by species-specific constraints that impose a maximal standing biomass per unit ground area K. These can be genetic constraints, e.g. the stem strength of a woody plant, the maximal biomass an annual life form can attain during its short life cycle, etc.. Temporal changes of the soil-water content are affected by the infiltration of surface water into the soil IH, by water loss due to biomass dependent evaporation or deep infiltration beyond the reach of the roots $-LW$, water uptake by plants' roots $-G_W W$, and by soil-water diffusion $D_W\nabla^2 W$. Finally, surface-water changes are affected by precipitation P, infiltration into the soil $-IH$, and overland water flow $-\nabla\cdot\mathbf{J}$, where the flux $\mathbf{J}$ depends on the ground surface height $\tilde{Z}(X,Y)$, which we describe in terms of the quantity $Z = \rho_w\tilde{Z}$, where ρ_w is the density of water. The quantity Z describes the landscape's topography. The equation for the surface water is a particular case of the diffusive-wave approximation of the shallow water equations [38]. Note that for flat terrains for which Z is constant the transport term $-\nabla\cdot\mathbf{J}$ reduces to $D_H\nabla^2(H^2)$.

The explicit form of the biomass dependence of the evaporation rate L is modeled as

$$L = \frac{N}{1+RB/K}, \tag{6}$$

where N is the evaporation rate in bare soil and R is a positive constant that quantifies the reduced evaporation by the plants' canopies and the litter they produce. The explicit forms of I, G_B and G_W are chosen so as to capture the various feedbacks discussed in the previous section. We have already introduced the form of the infiltration rate in (1). The term $-IH$ in (4c), which creates surface water gradients in the case of strong infiltration contrasts ($f \ll 1$), together with the overland water flow term $-\nabla\cdot\mathbf{J}$, and the water dependence of the biomass growth rate G_B (see below), account for the infiltration feedback.

The biomass growth rate G_B and the water uptake rate G_W are given by

$$G_B(\mathbf{X},T) = \Lambda\int_\Omega G(\mathbf{X},\mathbf{X}',T)W(\mathbf{X}',T)d\mathbf{X}',$$
$$G_W(\mathbf{X},T) = \Gamma\int_\Omega G(\mathbf{X}',\mathbf{X},T)B(\mathbf{X}',T)d\mathbf{X}', \tag{7}$$

where Λ is the biomass growth rate per unit soil-water content, Γ is the soil-water uptake rate per unit above-ground biomass, $G(\mathbf{X},\mathbf{X}')$ is the root kernel (2), which is determined by the root architecture of the particular plant species considered, and Ω is the lateral root zone. In the studies to be described we use the following Gaussian form for the root kernel:

$$G(\mathbf{X},\mathbf{X}',T) = \frac{1}{\pi S_0^2}\exp\left[-\frac{|\mathbf{X}-\mathbf{X}'|^2}{S[B(\mathbf{X},T])]^2}\right], \tag{8}$$

where $S_0 = S(0)$ represents the lateral root-zone size of a seedling. The nonlocal forms of G_B and G_W reflect the water uptake by laterally extended root systems. According to the form of G_B, the biomass growth rate depends not only on the amount of soil water at the plant location $\mathbf{X}$, but also on the amount of soil water at any point $\mathbf{X}'$ at the

Table 1
Dimensions of all quantities appearing in the model equations in terms of the fundamental dimensions: length ($\mathcal{L}$), mass ($\mathcal{M}$), and time ($\mathcal{T}$). We will use units of meters (m), kilograms (kg) and years (yr), respectively.

Quantity	Dimension
B, W, H, Z, K, Q	$\mathcal{L}^{-2}\mathcal{M}$
D_B, D_W	$\mathcal{L}^2\mathcal{T}^{-1}$
M, N, A	$\mathcal{T}^{-1}$
D_H	$\mathcal{L}^4\mathcal{M}^{-1}\mathcal{T}^{-1}$
Λ, Γ	$\mathcal{L}^2\mathcal{M}^{-1}\mathcal{T}^{-1}$
E	$\mathcal{L}^2\mathcal{M}^{-1}$
P	$\mathcal{L}^{-2}\mathcal{M}\mathcal{T}^{-1}$
T	$\mathcal{T}$
X, Y, S_0	$\mathcal{L}$
R, f	1

reach (Ω) of the plant's roots. Similarly, contributing to the water uptake rate G_W at a point $\mathbf{X}$ are plants located at distant points $\mathbf{X}'$ whose roots extend to $\mathbf{X}$.

The soil-water diffusion feedback is captured by choosing both E and the ratio D_W/D_B to be large enough. Large E is required to create strong local depletion of soil-water at the growing vegetation patch and steep soil-water gradients. Large D_W/D_B is required to guarantee fast soil-water diffusion towards the vegetation patch relative to patch expansion. Otherwise, patch expansion would act to smooth out the soil-water gradients and reduce the transport of water that is needed to maintain the positive feedback.

For simplicity, we have not presented the model Eq. (4) in their most general form. The linear soil-water (W) dependence of the biomass-growth and water-uptake terms is a simplification of a more realistic dependence of the form $W/(W_0+W)$, where W_0 is a half saturation constant [39]. It reduces to a linear dependence when $W \ll W_0$. Biomass loss has been associated with mortality, but other drivers of biomass loss exist, which require the introduction of non-constant biomass-decay rates, e.g. grazing stress which can be modeled by a biomass-dependent decay rate $M = M(B)$. The biomass "diffusion" term represents short-distance seed dispersal or clonal expansion, but can be generalized to describe long-distance seed dispersal by introducing a nonlocal term involving an integral over a kernel function [40,41]. The nonlocal term reduces to a diffusion term for sufficiently localized kernels. Finally, we have not included an evaporation term in the surface-water Eq. (4c), assuming a short residence time of surface water due to fast overland flow and high infiltration rates, especially in vegetation patches. When these conditions are not met an evaporation term similar to (6) should be included in (4c).

The dimensions of all quantities appearing in the model equations are given in Table 1. Note that although H and Z have dimensions of mass per unit area, we can regard H and Z as having dimensions of length by referring to the same quantities divided by the density of water, $\rho_w = 1$ g/cm^3. With this convention 1 kg /m^2 is equivalent to 1 mm and the precipitation rate P can be measured in units of millimeters per year (mm/yr).

Implicit in the model Eq. (4) are two additional assumptions. The first is that the landscape has a fixed topography. Thus, while past erosion-deposition processes, that shaped the topography, may have significant effects on water flow and vegetation growth, the latter processes are assumed to have no significant feedback on the topography [42]. The second assumption is that while rainfall may strongly affect vegetation growth, the total vegetation biomass is too small to feed back on the atmosphere and affect the rainfall [43].

2.3.2. A community of plants

The model Eq. (4) describe the dynamics of a single population of a given species. A straightforward extension of these Eq. (4) to describe a community of species leads to the following equations:

$$\partial_T B_i = G_B^i B_i(1 - B_i/K_i) - M_i B_i + D_{B_i}\nabla^2 B_i \tag{9a}$$

$$\partial_T W = IH - LW - W\sum_i G_W^i + D_W\nabla^2 W \tag{9b}$$

$$\partial_T H = P - IH - \nabla\cdot\mathbf{J}, \tag{9c}$$

where the index $i = 1,\ldots,n$ runs over the life forms that constitute the community, B_i stands for the above-ground biomass per unit ground area of the ith life form, and the overland water flux $\mathbf{J}$ is given by (5). The biomass dependence of the infiltration rate is a generalization of (1):

$$I = A\frac{\sum_i Y_i B_i + Qf}{\sum_i Y_i B_i + Q}, \tag{10}$$

where Y_i represents the contribution of the ith species to the increased infiltration rate in a vegetation patch and $Y_1 = 1$. Likewise the biomass dependence of the evaporation rate L is a generalization of (6) and reads

$$L = \frac{N}{(1+\sum_i R_i B_i/K_i)}. \tag{11}$$

Finally, the biomass-growth rate and the water-uptake rate given by (7) are generalized to

$$G_B^i(\mathbf{X},T) = \Lambda_i\int_\Omega G_i(\mathbf{X},\mathbf{X}',T)W(\mathbf{X}',T)d\mathbf{X}', \tag{12}$$

$$G_W^i(\mathbf{X},T) = \Gamma_i\int_\Omega G_i(\mathbf{X}',\mathbf{X},T)B_i(\mathbf{X}',T)d\mathbf{X}', \tag{13}$$

where

$$G_i(\mathbf{X},\mathbf{X}',T) = \frac{1}{\pi S_i^2}\exp\left[-\frac{|\mathbf{X}-\mathbf{X}'|^2}{[S_i(1+E_iB_i(\mathbf{X},T))]^2}\right]. \tag{14}$$

Plant species in water-limited systems often compete for sunlight in addition to water, as taller plants reduce the availability of light to shorter plants by shading. The positive feedback between shoot growth and light availability results in an inter-specific competition for light that can lead to the dominance of the taller plant species [44]. To capture this competition we introduce the following form for the biomass growth rate parameter that appears in (12) [45]:

$$\Lambda_i(B) = \Lambda_{0i}\left(1 - \frac{\Sigma_{j\neq i}B_j}{\Sigma_j B_j + B_R}\right). \tag{15}$$

Here, Λ_{0i} represents the growth rate of the ith life form in the absence of competitors and B_R is a positive constant serving as a reference value for the total biomass beyond which light becomes a limiting resource for small plants [46].

An important factor affecting community structure is grazing by herbivores, which acts to remove above-ground biomass mostly from tall plants with palatable leaf tissue [47–49]. We therefore model grazing as a biomass dependent term in the total biomass loss rate,

$$M_i = M_{0i} + M_{1i}B_i, \tag{16}$$

where M_{0i} is the biomass-loss rate of the ith species due to mortality and $M_{1i}B_i$ is the loss rate due to grazing.

Plant species differ from one another in many respects. Many of these differences can be captured by the trait parameters that appear in the model equations, such as growth rates (Λ_i), uptake rates (Γ_i), mortality rates (M_i), root-to-shoot ratios (E_i), maximal standing biomass (K_i), seed dispersal (D_{B_i}) and others. Characterizing the community by small volume elements in a space spanned by all trait parameters, however, requires solving the equations in a high-dimensional trait space, which is a formidable task. Instead, we may focus on selected response and effect traits. Considering biomass production as the ecosystem function of interest in a water-limited plant community, we choose the root-to-shoot ratio, E, as the response trait, and the maximum standing biomass, K, as the effect trait.

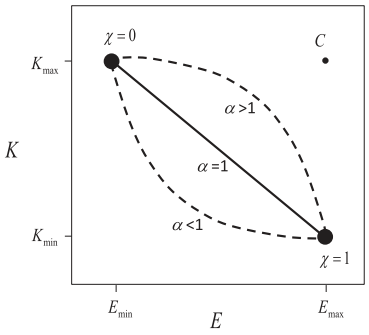

Fig. 4. Root-shoot ($E-K$) tradeoff curves obtained from (17) for three different α values. The big solid circles represent the two extreme tradeoff cases, $\chi=0$ and $\chi=1$. The small solid circle C represents an ideal case (both shoots and roots are long) that serves as a reference point - species described by tradeoff points that are closer to C have larger fitness.

We further assume that there is a tradeoff between these two traits; the plant's investment in above-ground biomass comes at the expense of investment in below-ground biomass and vice versa. This tradeoff allows the replacement of the two functional traits E and K by a single dimensionless tradeoff parameter, $0\le\chi\le 1$, defined implicitly through the relations

$$E(\chi)=E_{min}+\chi^{\alpha}(E_{max}-E_{min}),$$
$$K(\chi)=K_{min}+(1-\chi)^{\alpha}(K_{max}-K_{min}). \tag{17}$$

The parameter α describes different tradeoff curves in the K, E plane, as Fig. 4 shows, and may represent different species pools.

The parameter χ can be used to define the functional groups that comprise the community as follows. Discretizing χ uniformly along the interval [0,1]: $\chi_i=i/n$, $i=1,\ldots,n$, we define the ith functional group as the point χ_i and the small increment $\Delta\chi=1/n$ that precedes it. In the model Eq. (9) the ith functional group is described by a biomass variable B_i that satisfies (9) with $K_i=K(\chi_i)$ and $E_i=E(\chi_i)$, where all other parameters assume the same values for all functional groups. In general, there might be additional tradeoff parameters that characterize each functional group [50,51]. For simplicity, we will consider in the following a single tradeoff, focusing on the $E-K$ tradeoff (17) as an example [45,46].

2.3.3. Model simplifications

The general model Eq. (4) simplify considerably in two specific ecological contexts. The first refers to ecosystems with plant species whose roots are spatially confined in the lateral directions relative to the biomass and soil-water distributions. If both B and W are approximately constant across the narrow root zone, we can substitute $W(\mathbf{X}',T)\approx W(\mathbf{X},T)$ and $B(\mathbf{X}',T)\approx B(\mathbf{X},T)$ inside the integrals (7) and integrate the remaining Gaussian function over $\mathbf{X}'$:

$$\int_{\Omega}G(\mathbf{X},\mathbf{X}',T)d\mathbf{X}'=\frac{1}{\pi S_0^2}\left(\int_{-\infty}^{\infty}\exp\left(-\frac{X'^2}{S^2}\right)dX'\right)^2=s^2, \tag{18}$$

where $s=S(B)/S_0=1+EB$. Inserting this result in (7) we obtain the following local forms for the biomass-growth and water-uptake rates:

$$G_B=\Lambda W(1+EB)^2,\qquad G_W=\Gamma B(1+EB)^2. \tag{19}$$

The simplified model then consists of Eq. (4) with G_B and G_W given by (19). In this model only the infiltration and soil-water diffusion feedbacks are captured.

The second context that allows a considerable simplification of (4) is ecosystems with uncrusted sandy soil, where the infiltration rate in bare areas is as high as in vegetated areas. Assuming a biomass independent infiltration rate I, i.e. $f=1$ in (1), the equation for the surface water variable H decouples from those for B and W. This equation has a single stationary uniform solution, $H_0=P/I$, which is always linearly stable. Since H is the fastest variable we can assume that on the much longer time scales over which B and W significantly change it has already equilibrated at H_0. Inserting the solution $H=H_0$ into the equation for W, Eq. (4) reduce to the two-variable model

$$\partial_T B=G_B B(1-B/K)-MB+D_B\nabla^2 B, \tag{20a}$$

$$\partial_T W=P-LW-G_W W+D_W\nabla^2 W, \tag{20b}$$

where G_B and G_B are given by the non-local forms (7). This simplified model still captures two pattern-forming feedbacks, the root-augmentation and the soil-water diffusion feedbacks.

We can further combine the two simplifications made above to obtain a two-variable model with no integral terms, that is Eq. (20) with G_B and G_W given by (19). Out of the three pattern-forming feedbacks this simplification captures only the soil-water diffusion feedback. Similar simplifications can be applied to the model (9) for a plant community. In particular, the extension of (20) to a community consisting of n functional groups is

$$\partial_T B_i=G_B^i B_i(1-B_i/K_i)-M_i B_i+D_{B_i}\nabla^2 B_i, \tag{21a}$$

$$\partial_T W=P-LW-W\sum_i G_W^i+D_W\nabla^2 W, \tag{21b}$$

with

$$G_B^i=\Lambda_i W(1+E_i B_i)^m, \tag{22a}$$

$$G_W^i=\Gamma_i B_i(1+E_i B_i)^m, \tag{22b}$$

where Λ_i is given by (15) and we introduced the exponent m to distinguish between 1d systems for which $m=1$, and 2d systems for which $m=2$.

2.3.4. Non-dimensional equations

The model Eq. (4) can be brought to a non-dimensional form by scaling state variables, space and time coordinates and parameters as shown in Table 2. The advantages of this particular scaling is that four parameters are eliminated, K, M, Λ, S_0 (more than the three parameters that can be eliminated in an $\mathcal{LMT}$ system with three dimensionally independent parameters [12,52]), and the instability of the bare-soil state occurs at a critical precipitation value that is equal to unity ($p_c=1$) independently of any other parameter [36].

Expressed in terms of the non-dimensional quantities defined in Table 2, which include in particular the non-dimensional state variables (b, w, h) and the space and time coordinates ($\mathbf{x}$, t), the non-dimensional model equations are [36]:

$$\partial_t b=G_b b(1-b)-b+\delta_b\nabla^2 b, \tag{23a}$$

$$\partial_t w=\mathcal{I}h-lw-G_w w+\delta_w\nabla^2 w, \tag{23b}$$

$$\partial_t h=p-\mathcal{I}h-\nabla\cdot\mathbf{j}, \tag{23c}$$

Table 2
Relations between non-dimensional quantities and their dimensional counterparts.

Quantity	Scaling	Quantity	Scaling
b	B/K	p	$\Lambda P/MN$
w	$\Lambda W/N$	δ_b	D_B/MS_0^2
h	$\Lambda H/N$	δ_w	D_W/MS_0^2
q	Q/K	δ_h	$D_H N/M\Lambda S_0^2$
ν	N/M	ζ	$\Lambda Z/N$
α	A/M	ρ	R
η	EK	t	MT
γ	$\Gamma K/M$	$\mathbf{x}$	$\mathbf{X}/S_0$

with

$$\mathbf{j} = -2\delta_h h \nabla(h+\zeta). \tag{24}$$

Here, the non-dimensional evaporation rate l, infiltration rate $\mathcal{I}$, growth rate G_b and soil-water uptake rate G_w are given by

$$l = \frac{\nu}{1+\rho b}, \qquad \mathcal{I} = \alpha \frac{b(\mathbf{x},t)+qf}{b(\mathbf{x},t)+q}, \tag{25}$$

$$G_b(\mathbf{x},t) = \nu \int_\Omega g(\mathbf{x},\mathbf{x}',t) w(\mathbf{x}',t) d\mathbf{x}',$$

$$g(\mathbf{x},\mathbf{x}',t) = \frac{1}{\pi} \exp\left[-\frac{|\mathbf{x}-\mathbf{x}'|^2}{\tilde{s}[b(\mathbf{x},t)]^2} \right], \tag{26}$$

and

$$G_w(\mathbf{x},t) = \gamma \int_\Omega g(\mathbf{x}',\mathbf{x},t) b(\mathbf{x}',t) d\mathbf{x}', \tag{27}$$

where $\tilde{s}(b) = s(B)$ and the dimensionless counterpart of E is

$$\eta = \frac{d\tilde{s}}{db}|_{b=0} = \frac{ds}{dB}|_{B=0} K = EK. \tag{28}$$

The non-dimensional form of the precipitation parameter

$$p = \frac{\Lambda P}{MN}, \tag{29}$$

shows the equivalence of decreasing the precipitation rate, P, to increasing the mortality rate, M, or the evaporation rate, N. Similar scaling relationships can be applied to the community version of the model [37] and to the simplified versions of the model [53].

3. Pattern formation links

The platform of models introduced in the previous section can be used to study various relationships between pattern formation, on one hand, and the abiotic environment, biodiversity and ecosystem function, on the other hand. We briefly describe several examples of such relationships and refer the reader to the relevant literature for detailed accounts.

3.1. Pattern formation and the abiotic environment

As pointed out earlier, vegetation pattern formation is a population-level means of an ecosystem to cope with an environmental stress. Depending on environmental conditions, the asymptotic patterns that form can be periodic, non-periodic or scale free, as we discuss in Sections 3.1.1–3.1.3 below. Quite often observed patterns do not represent asymptotic states. This is because of the relatively long time scales involved and because of disturbances as we discuss in Section 3.1.4. The model studies to be described have been carried out for a homogeneous system (no explicit space dependence in the model equations), and mostly for time-independent precipitation rates that represent mean annual rainfall. For studies of vegetation pattern formation in non-stationary and heterogeneous environments we refer the reader to the available literature on this subjects [54–61].

3.1.1. Basic vegetation states along the rainfall gradient

Consider the model Eq. (23) for a flat terrain, for which $\zeta = const.$ and

$$-\nabla \cdot \mathbf{j} = \delta_h \nabla^2(h^2), \tag{30}$$

and assume first a 1d system. The equations have two stationary uniform solutions representing physical states[2], bare soil ($b = 0$) and uniform vegetation. As the bifurcation diagram in Fig. 5 shows, the bare-soil solution is stable at low precipitation values p and loses stability in a uniform stationary instability at $p_c = 1$[3]. At this point a solution branch representing uniform vegetation appears. This solution branch is often unstable when it appears but becomes stable at high precipitation values that exceed a second threshold, p_2. As p is decreased below p_2 the uniform vegetation solution loses stability in a nonuniform stationary instability. At this point a solution branch representing stationary periodic vegetation patterns appears. Depending on parameters, the periodic biomass and soil-water distributions can be in phase or anti phase [53]. Its wave-number k_c can be calculated using a linear stability analysis [36]. This solution branch terminates on the uniform vegetation solution branch at a lower p value. Additional periodic solution branches appear below p_2 with decreasing wavenumbers, as Fig. 5 shows. They extend down to a precipitation threshold $p_1 < p_c$ below which the lowest wavenumber solution disappears in a fold bifurcation [39,62–64]. Note that these periodic solutions extend to precipitation values much lower than the uniform vegetation solution, highlighting the role of vegetation pattern formation as a population-level means of coping with water stress.

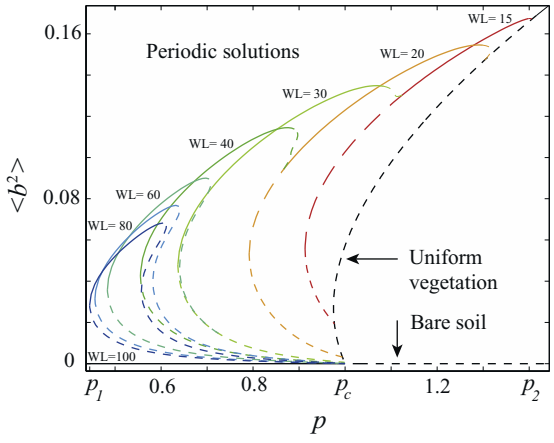

Fig. 5. A bifurcation diagram for (23) with G_B and G_W given by (19) in 1d. The vertical axis represents the spatial average of b^2 while the horizontal axis represents the precipitation rate. The diagram shows the existence and stability information for uniform vegetation and bare soil solutions, and for periodic solutions that differ in their wavelengths (WL) as indicated. From [12].

In 2d isotropic systems a continuous family of growing modes appear at $p = p_2$, with wave-vectors $\mathbf{k}$ spanning the circle $|\mathbf{k}| = k = k_c$. According to pattern formation theory [12,14,15,65,66], out of this family a triad ($\mathbf{k}_1$, $\mathbf{k}_2$, $\mathbf{k}_3$) of resonating modes, satisfying $\mathbf{k}_1 + \mathbf{k}_2 + \mathbf{k}_3 = \mathbf{0}$, is generally selected. The simultaneous growth of these modes gives rise to stable hexagonal solutions, which in the present context describe hexagonal patterns of vegetation gaps. Solution branches describing vegetation stripe patterns, e.g. with wavevector $\mathbf{k}_1$, also appear below $p = p_2$, but they are unstable to the growth of the resonating modes $\mathbf{k}_2$ and $\mathbf{k}_3$. Stable stripe patterns appear only at lower p values, and at yet lower p values stable hexagonal patterns of vegetation spots appear. Altogether five basic vegetation states can be distinguished along the rainfall gradient as Fig. 6 illustrates: uniform vegetation, hexagonal gap pattern, stripe pattern, hexagonal spot pattern and bare soil [36]. This is a universal sequence of states [67] that has been found in other contexts too. These predictions are consistent with empirical observations in water-limited regions throughout the world [8]. Observations of the three basic patterns, spots, stripes and gaps (for different species) are shown in Fig. 7.

[2] We use the term "uniform solution" to denote a spatially homogeneous solution.

[3] By uniform (nonuniform) stationary instability we mean an instability at which the first mode to grow has a zero (nonzero) wavenumber k and the growth is monotonic in time.

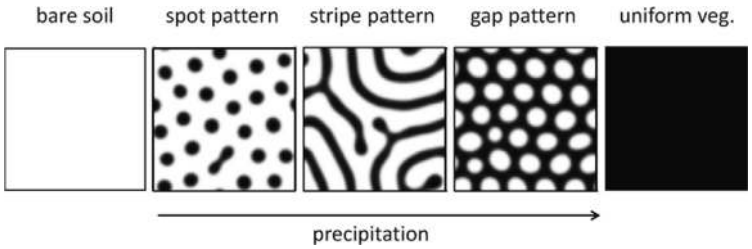

Fig. 6. The five basic vegetation states along the rainfall gradient; uniform vegetation, hexagonal gap pattern, stripe pattern, hexagonal spot pattern and bare soil. The pattern states shown are numerical solutions of (23)–(27). From [12].

Fig. 7. Aerial photographs of nearly periodic vegetation patterns in nature: (a) a spot pattern in Zambia (from [23]), (b) a stripe pattern in Niger (from [7]), (c) a gap ("fairy circle") pattern in Namibia. From [12].

Consider now a landscape with a constant slope in the x direction for which $\nabla\zeta = c\hat{\mathbf{x}}$, where c is the slope. The flow term in (23c) then becomes

$$-\nabla\cdot\mathbf{j} = \delta_h\nabla^2(h^2) + 2\delta_h c\partial_x h. \tag{31}$$

Studies of (23) with (31) leads to the same uniform solutions as for flat terrains, but the periodic pattern states differ in two main respects: (i) the stripe (or band) patterns orient themselves in a direction perpendicular to the slope, (ii) they migrate uphill [36,68]. The orientation perpendicular to the slope direction is a mean by which the vegetation maximizes the amount of water it receives by runoff interception; patterning along the slope would result in water leakage out of the system and vegetation decay. These findings have been found with simpler models too [18,69–71], and have been reported in field observations [72]. The effect of the slope on the pattern's wavelength has also been studied and found to be history dependent; patterns generated by degradation of uniform vegetation show increasing wavelengths with slope, whereas colonization of bare ground gives the opposite trend [73].

3.1.2. Localized structures and disordered patterns

The instability of uniform vegetation to periodic gap patterns is often subcritical, implying a precipitation range where two alternative stable states coexist, uniform vegetation and gap patterns. Under this condition many additional nonuniform stable solutions may exist; they describe confined domains (localized structures) of the patterned state of increasing sizes in a system otherwise occupied by the uniform vegetation state, and vice versa. This dynamical behavior, commonly referred to as *homoclinic snaking* [74,75], is related to the pinning of the fronts that separate adjacent domains of the two alternative stable states in a range of the control parameter [76][4]. Homoclinic snaking has indeed been found in the simplified model Eq. (20), which describe a particular ecosystem - the *Namibian Fairy-Circle* ecosystem [77,78]. Fairy circles are barren circular gaps in a grassland that form nearly periodic gap patterns. The confined domains amount in this context to groups of missing gaps in a periodic gap pattern, or to groups of gaps in a uniform grassland. Confined domains or localized structures also act as building blocks for a wide variety of disordered extended solutions. We call the localized and extended solutions *hybrid states* to distinguish them from the uniform-vegetation state and the periodic gap patterns [63].

Another bistability range of uniform and patterned states exists at a lower precipitation range – uniform bare-soil and periodic spot patterns. The behavior in this bistability range, however, is quite distinct from that described above for the bistability of uniform vegetation and periodic gap patterns, and is apparently related to the fact that the periodic-pattern solutions do not bifurcate from the uniform bare-soil solution, but rather from the uniform-vegetation solution. In this case, homoclinic snaking has been found only when a second bistability range of uniform vegetation and periodic patterns exists in the vicinity of the instability point, $p = p_c$, of the bare soil solution [78]. This bistability range is generally very small, if it exists, and the homoclinic snaking range is small too. Nevertheless, single-hump or single-spot localized solutions do exist in a wide precipitation range [64] and serve as building blocks for a variety of disordered extended patterns. Strictly speaking, the latter patterns are not asymptotic [79], but can be considered as such on ecological time scales.

3.1.3. Scale-free patterns

So far we discussed three basic periodic patterns (spots, stripes, gaps) and a variety of additional non-periodic patterns in bistability ranges of uniform and patterned states. Despite the wide variety of these patterns they all share one property – a characteristic length scale, whether it is the width of a stripe, the diameter of a spot or the diameter of a gap. Empirical studies in the Kalahari desert [80] and in Mediterranean ecosystems [81], however, have reported the observations of patterns with wide patch-size distributions, lacking any characteristic length. Studies of the model Eq. (23) show that such "scale-free" patterns can appear when the competition for water becomes global [80,82,83]. Global competition in the model equations can develop when the spatial distribution of the water resource is fast relative to processes that exploit it. A possible realization of this principle is fast surface-water flow relative to the infiltration of surface water into the soil [83], as discussed below.

Consider a system with a sharp infiltration contrast for which the infiltration feedback is the only driver of vegetation patchiness. When the condition of fast surface-water flow relative to infiltration is not satisfied, a small initial patch either grows to a vegetation spot of a characteristic size, or forms an expanding vegetation ring of a characteristic width [56,84]. Ring formation is a result of central dieback; when a growing vegetation patch becomes too large the surface water flowing toward it infiltrates mostly at the patch periphery and does not reach the patch center. Imagine now that the condition of fast surface-water flow relative to infiltration is satisfied. Then, by the time any significant infiltration takes place at a growing vegetation patch, surface water has already reached the patch center. As a result, central dieback is avoided and big patches can develop. Furthermore, at any vegetation patch where infiltration begins to take place, fast long-range overland flow immediately compensates for the local surface-water depletion, thereby inducing global competition. As a result, available surface water in the vicinity of a small patch can be exploited by farther bigger patches, preventing the growth of the

[4] This is unlike bistability of uniform states where fronts propagate in general and can only be stationary in a particular value of the control parameter, or because of a repulsive interaction with another front.

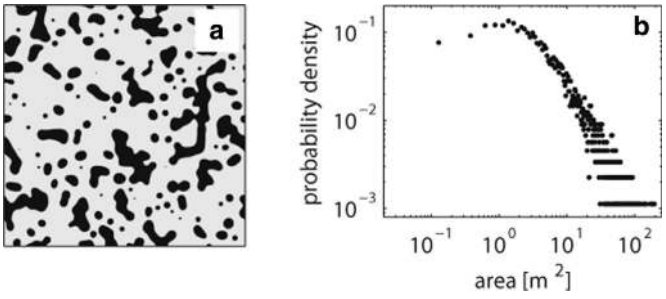

Fig. 8. A typical scale-free pattern, obtained for global competition induced by fast surface-water flow relative to infiltration (a), and the corresponding patch-size distribution (b). For additional information see Ref. [83].

small patch. The combination of these processes acts to maintain both large and small patches and therefore leads to wide patch-size distributions. A dimensional analysis [12] gives the following scaling relation for the ratio, ξ, between the areas occupied by the largest and smallest patches, S_{max} and S_{min}:

$$\xi = \frac{S_{max}}{S_{min}} \sim \frac{\sqrt{D_H P}}{A S_0}. \tag{32}$$

Model studies with $\xi \gg 1$ indeed show the possible appearance of wide patch-size distributions [83] as Fig. 8 indicates. They also show a slow process of patch coarsening [85], reminiscent of Ostwald ripening in two-phase mixtures [86].

3.1.4. Transient patterns

Many of the patterns seen in natural landscapes do not coincide with the asymptotic patterns predicted by the models, but can be interpreted as transients towards these asymptotic patterns, be they periodic or localized. A common transient pattern is the ring, various natural realizations thereof are shown in Fig. 9. As pointed out in Section 3.1.3, rings can result from central vegetation dieback as initially small spots grow in size. The dynamics of such spots depends on organismic parameters, such as the root-to-shoot ratio η, and on environmental parameters, such as the precipitation p. An initially small spot will approach a fixed size, rather than form a ring, when η is sufficiently large or p is sufficiently small. Under such conditions the growing spot significantly depletes the soil-water content in its neighborhood as Fig. 10a shows. At that level further spot expansion becomes impossible. By contrast, when η is sufficiently small, the rate of water uptake relative to the precipitation rate is too small to prevent spot expansion and ring formation as the water distribution shown in Fig. 10b suggests.

Two dieback mechanisms have been studied using (23) [56]. The first mechanism pertains to conditions of high infiltration contrast between vegetated and bare soil, under which overland water flow is intercepted at the patch periphery. The decreasing amount of water that the patch core receives as the patch expands, leads to central dieback and ring formation. The second mechanism pertains to plants with large lateral root zones, and involves central dieback and ring formation due to increasing water uptake by the new vegetation at the patch periphery. In general the two mechanisms act in concert, but the relative importance of each mechanism depends on environmental conditions; strong seasonal rainfall variability favors ring formation by the overland-flow mechanism, while a uniform

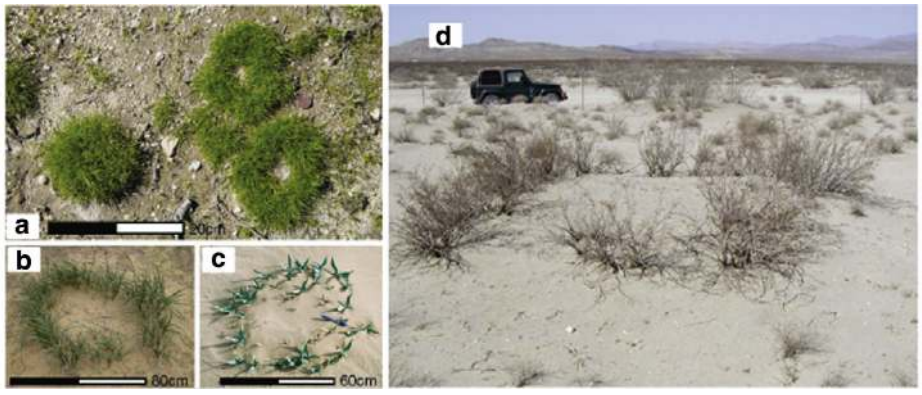

Fig. 9. Ring patterns in nature. (a) Mixtures of rings and spots of Poa bulbosa L. observed in the Northern Negev, Israel (150 mm/yr); (b) An Asphodelus ramosus L. ring observed in the Negev desert, Israel (170 mm/yr); (c) A ring of Urginea maritima (L.) Baker observed in Wadi Rum, Jordan (50 mm/yr); (d) Ring of Larrea Tridentata (DC.) Coville in Lucerne Valley, California, USA (98 mm/yr). From [56].

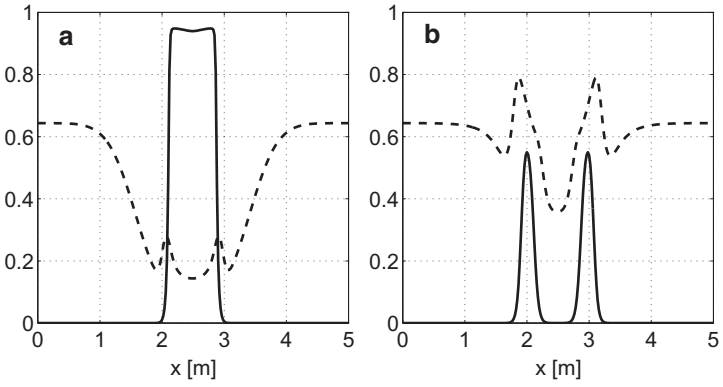

Fig. 10. Transects of two-dimensional spatial distributions of biomass (solid lines) and soil-water density (dashed lines) for (a) a stationary spot solution ($\eta = 3.2$), and (b) an expanding ring solution ($\eta = 1.6$). From [87].

rainfall regime favors ring formation by the water-uptake mechanism. These results explain the formation of rings by fast-growing species with confined root zones in a dry-Mediterranean climate, such as *Poa bulbosa*. They also explain the formation of rings by slowly-growing species with highly extended root zones, such as *Larrea tridentata* (Creosotebush) [56].

The mechanisms described above are based on biomass-water relations only. Other mechanisms have been proposed too, including a negative feedback between sediment deposition and vegetation growth [88] and the release of toxic materials [89,90]. For a recent review see Ref. [91]. We further note that rings generally develop on a fairly flat ground; on a slope crescent shapes develop instead [87].

3.2. Pattern formation and ecosystem function

Ecosystem function is often impaired by transitions from one stable system state to an alternative stable state. Such transitions, commonly referred to as "regime shifts" [92], are generally conceived as abrupt events occurring uniformly across the ecosystem. The transitions can be induced by varying environmental conditions that move the system across an instability point or by disturbances that kick the system out of the attraction basin of its current state. This view overlooks significant pattern formation aspects [93], which we discuss in Section 3.2.1 in the context of desertification. The reciprocal process of restoring degraded landscapes and ecosystem function can be viewed as a spatial resonance problem, and is discussed in Section 3.2.2.

3.2.1. Desertification

Regime shifts that involve loss of biological productivity represent forms of desertification. They are particularly relevant to water-limited ecosystems where multi-stability of states is predicted by model studies and implied by field observations [10]. The simplest realization of alternative stable states that can be envisaged in such ecosystems is bistability of a uniform vegetation state and a uniform bare-soil state. Bistability of this kind can be obtained with non-pattern-forming positive feedbacks, such as reduced evaporation rate of above- and below-ground water in vegetated areas compared to bare soil, and increase of nutrient concentration as a result of litter decomposition. More common, however, is bistability of uniform and patterned states, either uniform vegetation and gap patterns or uniform bare soil and spot patterns.

The simple view of regime shifts overlooks the possible occurrence of spatially confined disturbances, which can induce local transitions to the alternative stable state, and nonuniform instabilities to spatially periodic patterns. Consider first the simplest case of bistability of uniform states and an ecosystem in one of these states, which is disturbed by confined domains of the alternative state. The subsequent dynamics of such a state are determined by the properties of the fronts that bound these domains. These fronts generally propagate at a unique velocity. Varying the control parameter across the bistability range results in a change of the direction of front propagation at the so-called Maxwell point. Depending on which side of the Maxwell point the system is, confined domains of the alternative state either contract and disappear, or expand and gradually induce a global shift to the alternative stable state [93]. Unlike abrupt regime shifts, gradual shifts of this kind can occur far from any instability point. As a consequence, early warning signals for impending shifts that are based on the proximity to instability points [94] are not applicable. Note, though, that the closer the system to the Maxwell point the slower is the global shift. Thus, although the Maxwell point designates a sharp borderline between recovery from a disturbance and gradual shift [95], traversing this point does not involve any sharp dynamical change.

At least two exceptions to this simple behavior should be noted. Repulsive front interactions can prevent the coalescence of two domains approaching one another and can result in asymptotic spatial patterns. This is often the case in activator-inhibitor systems with fast inhibitor diffusion [96], and may be relevant to water limited ecosystems with fast water transport. Another exception pertains to non-gradient systems which go through a "Nonequilibrium Ising-Bloch" (NIB) bifurcation. This is a front bifurcation that results in a pair of stable counter-propagating fronts. Beyond the NIB bifurcation, confined domains of the alternative stable state may induce persistent spiral waves, and in the vicinity of the NIB bifurcation a state of spatio-temporal chaos, nurtured by repeated events of spiral-pair nucleation, may result [97–101].

Nonuniform instabilities of uniform states lead to bands of stable periodic solutions, and this holds for the instability of the uniform vegetation state too. As the precipitation rate is decreased new periodic solutions with successively longer wavelengths appear, as Fig. 5 shows [63,102]. Desertification may therefore involve gradual transitions to successively sparser periodic patterns before an abrupt transition to bare soil takes place [64].

The nonuniform instability of the uniform vegetation state is often subcritical (for parameters representing realistic contexts), and leads to a bistability range of uniform vegetation and periodic patterns. This allows for yet another response form to rainfall variability. As discussed in Section 3.1.2, when one of the alternative stable states is spatially patterned a subrange of the bistability range may exist where fronts do not propagate but are rather pinned in place. Within this subrange a multitude of stable hybrid states exist. Local disturbances within the hybrid-state subrange result in the convergence to stable hybrid states with no further dynamics, unlike the case of two uniform alternative states. However, environmental variability can induce rich dynamical behaviors [103]. In particular, an asymmetric variability, such as a series of droughts, can induce gradual desertification from a disturbed uniform-vegetation state to a periodic-pattern state [78,93]. This will be the case when the droughts are strong enough to take the system out of the hybrid-state subrange where fronts are no longer pinned and the periodic pattern state propagates into the uniform-vegetation state. A good candidate ecosystem for observing and studying gradual desertification of this kind is the Namibian fairy-circle ecosystem, where fairy-circle birth and death processes can be interpreted as instances of front propagation [78].

3.2.2. Resilience of restored landscapes

How can desertification be reversed once it has occurred? A common practice is water harvesting by spatially periodic ground modulations, often in the form of parallel linear embankments, that intercept overland water flow and along which vegetation is planted [104]. Various open questions arise in regard to this practice: how far apart should the linear embankments be? Should the vegetation be planted continuously along the embankments? How should particular choices of ground-modulation templates and planting patterns affect ecosystem function in terms of biological productivity and resilience to environmental variability?

Since water-limited vegetation tends to self-organize in spatial patterns even in the absence of a ground-modulation template, the practice of water-harvesting is, in essence, a spatial resonance problem; the success of this practice depends on the system's ability to yield to the imposed template of ground modulations. The response of pattern-forming systems to periodic spatial forcing [105–110], periodic ground modulations in the present context, has been the subject of active research recently [111–123]. We focus here on one aspect of these studies that is relevant to the question of the resilience of restored vegetation to rainfall variability [124]. Periodic ground modulations can be captured in the model Eq. (23) by modulating the topography function ζ to simulate embankments, or by modulating the infiltration parameter f, which amounts to a template of crust removal.

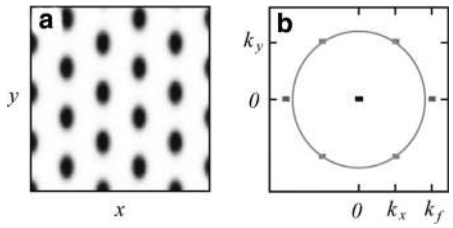

Fig. 11. A resonant rhombic pattern in the vicinity of the 1:1 resonance of stripe patterns ($k_f = 1.1k_0$). Panel (a) shows the biomass distribution in the x, y plane of a solution of (23) with a periodically modulated infiltration rate given by (34). Panel (b) shows the power spectrum of the solution relative to the circle $|\mathbf{k}| = k_0$, where darker dots denote higher power. The four peaks on the circle of radius k_0 representing two oblique modes, $\mathbf{k}_{\mp} = (-k_x, \mp k_y)$, and their complex conjugates, $-\mathbf{k}_{\mp}$. The value $k_x = k_f/2$ indicates that the 2d patterns is resonant. For further information see Ref. [124].

Two-dimensional (2d) systems do not necessarily follow stripe-like periodic forcing; rather than forming 1:1 resonant stripe patterns [112], which in the restoration context amounts to a vegetation band along each embankment or stripe of removed crust, they often respond by forming 2d resonant rhombic patterns. That is, if the forcing wave-vector is $\mathbf{k}_f = (k_f, 0)$ (i.e. oriented along the x direction) and the wave-number of the preferred mode in the unforced system is k_0, the power spectra of the patterns that form contain three major modes: two oblique modes with wave-vectors

$$\mathbf{k}_{\mp} = (-k_x, \mp k_y), \quad k_x = k_f/2, \quad k_y = \sqrt{k_0^2 - k_x^2}, \tag{33}$$

and a stripe mode $\mathbf{k}_f = (\pm k_f, 0)$. These modes resonate with the forcing and satisfy the resonance condition $\mathbf{k}_+ + \mathbf{k}_- + \mathbf{k}_f = 0$ in a wide range of forcing wave-numbers, k_f. This is because of the freedom of the system to select the wave-vector component k_y such that the total wave-number of each of the oblique modes is the preferred one, $k_- = k_+ = \sqrt{k_x^2 + k_y^2} = k_0$ (see Eq. (33)). This makes the pattern robust even in the vicinity of the 1:1 resonance where $k_f \approx k_0$ [116,124].

Fig. 11 shows an example of a resonant rhombic pattern in the vicinity of the 1:1 resonance of stripe patterns ($k_f = 1.1k_0$) and the corresponding power spectra. The solution shown was obtained by solving numerically a simplified version of (23), in which the only pattern forming mechanism is the infiltration feedback, with periodic modulation of the infiltration parameter

$$f = f_0\left[1 + \frac{\gamma_f}{2}(1 + \cos(k_f x))\right]. \tag{34}$$

Rhombic patterns of this kind destabilize resonant stripe patterns at sufficiently low precipitation and extend as stable solutions to precipitation values below the existence range of stripe solutions. This result bears on the preferred restoration pattern in terms of resilience to precipitation downshifts as we now discuss.

Starting from a precipitation range where 1:1 resonant stripe patterns are stable, precipitation downshifts to values below this range can lead to two distinct behaviors, convergence to resonant rhombic patterns and collapse to bare soil. The former behavior is obtained with relatively small downshifts, where resonant stripes solutions still exist as unstable solutions, while the latter behavior occurs with larger downshifts where resonant stripe solutions no longer exist. The reason for this dramatic change in the response of the system as the unstable stripe solutions disappear is that their unstable manifold, which represents the growth of the oblique modes and the convergence to rhombic patterns, acts as a barrier for the flow in phase space and prevents the approach to the stable bare-soil state. This constraint on the flow no longer exists when the unstable stripe solutions cease to exist. The conclusion from this study is that restoration in stripe patterns is not resilient to rainfall variability and may result in a complete failure. Restoration in rhombic patterns, which involve discontinuous plantation along the ground modulations, does not suffer from this problem. Furthermore, upon precipitation upshifts rhombic patterns converge smoothly to stripe patterns [124]. Restoration in resonant rhombic patterns is therefore advantageous over the more intuitive restoration in resonant stripe patterns.

3.3. Pattern formation and biodiversity

Associated with self-organized vegetation patterns are nonuniform soil-water distributions. The redistribution of the water resource by a pattern-forming plant species can change interspecific interactions. The magnitude of this effect depends on the relative strength of different pattern-forming feedbacks, on the rainfall regime and on the actual spatial patterns being formed, as discussed in Section 3.3.1. The changes in interspecific interactions, along with environmental filtering, can affect community-level properties such as functional diversity, community composition and others. These effects, however, have hardly been studied using a mathematical-modeling approach; the limited progress that has been made is discussed in Section 3.3.2.

3.3.1. Plants as ecosystem engineers

An important concept in the study of interspecific interactions is that of an *ecosystem engineer* [125,126]. An ecosystem engineer is an organism that affects the growth of other organisms by modifying the abiotic environment. Numerous examples of organisms that act as ecosystem engineers exist [127]. In dryland plant communities, ecosystem engineering has been studied mostly in the context of shrubs and herbs that grow in the vicinity of and under the shrub canopy [128,129]. Using the single-species model (23), we can first explore the capacity of a woody life form to act as an ecosystem engineer. The soil-water content in a vegetation patch, as compared with the content in bare soil, strongly depends on the relative strength of the infiltration and root-augmentation feedbacks. While the infiltration feedback acts to increase the soil-water content by overland water flow toward the patch, the root-augmentation feedback acts to deplete it by strong water uptake. Thus, strong infiltration feedback and weak root-augmentation feedback lead to high soil-water concentration in the vegetation-patch area, whereas weak infiltration feedback and strong root-augmentation feedback lead to soil-water depletion in the patch area and its surroundings [36]. By concentrating the water resource beyond the bare-soil level, the woody life form creates an ameliorated micro-environment that may increase the fitness of other plant species and result in higher species richness [10,37].

Ecosystem engineering, however, depends on additional factors besides the relative strength of the two feedbacks. For a given woody life form it can change along the rainfall gradient and for a fixed environment it can change with the spatial pattern that the woody plant forms [37]. The relation between ecosystem engineering and water stress is demonstrated by the single life-form simulations shown in panels a and b of Fig. 12. At relatively high precipitation a typical vegetation patch is big, the water uptake from any area element within the patch is high and the patch is dryer than the surrounding bare soil (Fig. 12b). By contrast, at sufficiently low precipitation the patches are small and the uptake is low, while the infiltration rate remains high in areas that are still covered by vegetation. As a result, the increase of soil-water content in any area element within the patch by infiltration exceeds the decrease by water uptake and the patch becomes wetter than the surrounding bare soil (Fig. 12a). Thus, while at high precipitation the woody life form excludes the herbaceous life form, at low precipitation it acts as an ecosystem engineer and can facilitate the growth of the herbaceous life form, as panels c and d in Fig. 12 show.

Fig. 13 shows the effect of spatial patterning on ecosystem engineering; while in a sparse, savanna-like pattern the woody life form

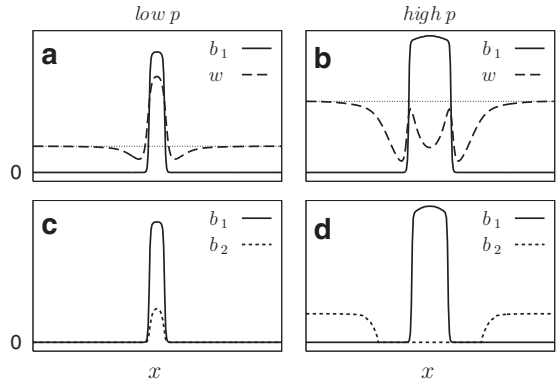

Fig. 12. Model solutions showing the development of ecosystem engineering as precipitation decreases. Panels a and b show spatial profiles of the biomass b of a woody ecosystem engineer and of the soil-water content w, at low and high precipitation rates, using the model equations for a single life form. Panels c and d show the corresponding responses of a herbaceous life form to the ecosystem engineering of a woody life form, obtained by solving the model equations for two life forms. While at high precipitation the woody life form excludes the herbaceous life form, at low precipitation the woody life form facilitates the growth of the herbaceous life form. For further information see [37].

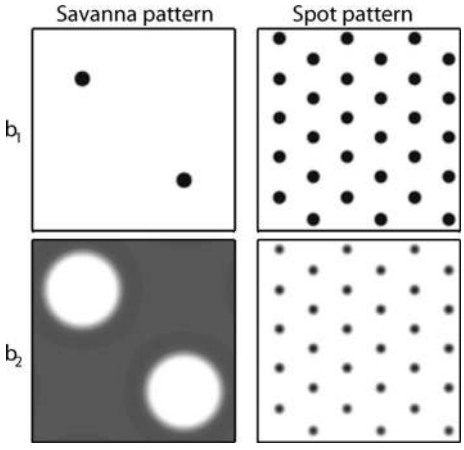

Fig. 13. Model solutions showing the development of ecosystem engineering with pattern density. The panels on the left show a savanna-like pattern with two isolated woody patches (b_1) in an otherwise uniform herbaceous vegetation (b_2). In this case the woody life form excludes the herbaceous life form. The panels on the right show a dense spot pattern at the same parameter values. In this case the woody life form facilitates the growth of the herbaceous life forms. For further information see [37].

excludes the herbaceous life form, in a dense spot pattern it facilitates the growth of the herbaceous life form understorey. Ecosystem engineering can therefore develop in dense woody patterns.

3.3.2. Community-level properties

In order to study how changes in interspecific interactions affect community structure, we first need a method of deriving community-level properties. Consider the simplified model Eq. (21) and (22), for a community consisting of n functional groups uniformly distributed along the tradeoff axis χ (see Section 2.3.3). In order to relate model findings to field observations in annuals' communities, we will regard the functional groups as describing herbaceous life forms. It will be useful to view the n biomass variables B_i, $i = 1, \ldots, n$ as discretized values of a continuous biomass function, $B = B(\mathbf{X}, \chi, T)$, with $B_i = B(\mathbf{X}, \chi_i, T)$. Fig. 14 shows a typical asymptotic form of such a function obtained by solving (21) numerically for a non-pattern-forming community for which the state variables are space independent [46]. The pulse-shape form of the biomass distribution along the tradeoff axis contains information about three community-level properties: functional diversity (pulse width), community abundance (pulse area) and community composition (pulse position). Note that

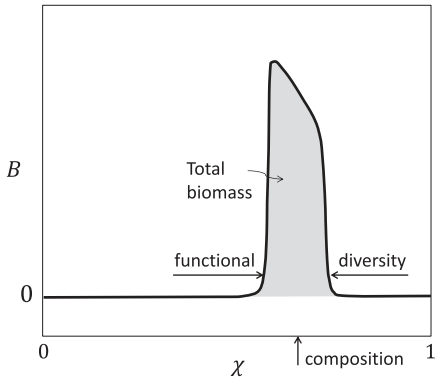

Fig. 14. A typical pulse-shape biomass solution of (21). The biomass distribution along the tradeoff axis χ contains information about functional diversity (pulse width), composition (pulse position) and total biomass (pulse area).

these properties can be related to the low moments of the biomass distribution [130].

A variety of additional community level properties can be derived by studying pulse solutions of this kind along environmental gradients. As an example, we show in Fig. 15 a relation between functional diversity and precipitation, and how it is affected by a grazing stress [46]. Note first that the relation is monotonically increasing. Note also the negative effect of grazing on diversity at low precipitation and the positive effect at high precipitation. This behavior supports the *grazing reversal hypothesis*, which attributes the positive effect of grazing at high precipitation to selective grazing of tall plants. This results in reduced competitive exclusion by the tall plants and the coexistence of short, less competitive plants, and in overall higher diversity.

The composition of the community changes too along the rainfall gradient [46]. Following a phase of environmental filtering, where new functional groups that specialize both in water capture and in light capture are added to the community as the precipitation is increased, a competition phase begins in which functional groups that specialize in capturing water (high χ groups) are displaced by functional groups that specialize in capturing light (low χ groups).

The community-level properties discussed so far apply to spatially uniform communities. How does spatial variability induced by pattern-forming instabilities affect community dynamics? Since pattern formation increases the ability of a functional group to cope with water stress, the existence of pattern-forming functional groups in the community should affect the manner by which community structure changes along a rainfall gradient.

The effect of pattern formation, however, can be more intricate, as it can couple different functional groups. As an example consider a small community in 1d consisting of two functional groups, one specializing in capturing light, $\chi = 0$, with biomass B_1, and the other in capturing water, $\chi = 1$, with biomass B_2. As the bifurcation diagram in Fig. 16 shows, a precipitation range can be identified with two stable pure population states, a spatially periodic $\chi = 0$ state, $U^*_{1,p} = (B^*_1(x), 0, W^*_1(x))$, and a uniform $\chi = 1$ state, $U^*_2 = (0, B^*_2, W^*_2)$. This bistability range of uniform and patterned states gives rise to homoclinic snaking and to a wide variety of hybrid states representing spatial coexistence of the two functional groups, as Fig. 17 shows. Locally, each group excludes one another (see insets a-d in Fig. 17), but neither group can displace the other because of front pinning. Thus, pattern formation can affect community structure by forming stable mosaics of different functional groups and thereby spatial coexistence.

4. Discussion

We described examples of several processes that link pattern formation to aspects of the abiotic environment, biodiversity and

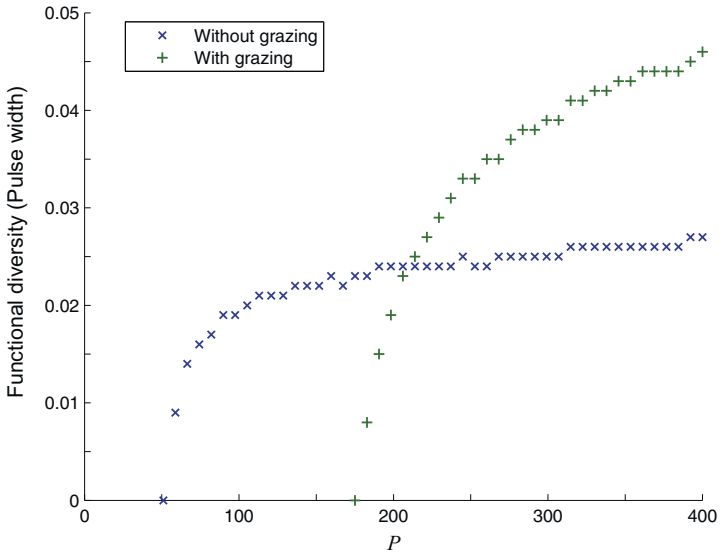

Fig. 15. Diversity-precipitation relations for plant communities that are subjected (plus curve) and not subjected (cross curve) to grazing stress.

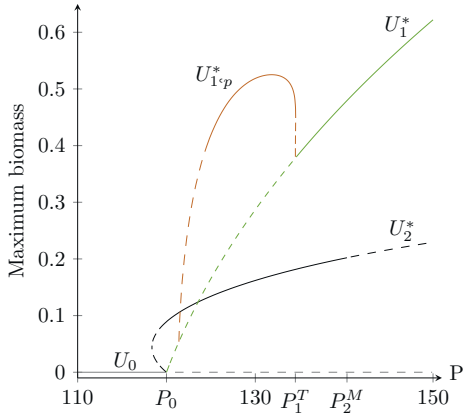

Fig. 16. Bifurcation diagram for a system of two life forms, $\chi = 0$ with biomass B_1 and $\chi = 1$ with biomass B_2. The diagram shows the biomass-precipitation solution branches for the bare-soil state, U_0, the two pure-population uniform states, U_1^* and U_2^*, and for the pure-population periodic-pattern state, $U_{1,p}^*$, for which the maximum biomass is plotted. The two uniform states bifurcate from the bare-soil state at $P = P_0$. The periodic-pattern state bifurcates from the corresponding uniform state at $P = P_1^T$ and reconnects to it at a lower precipitation value. From [45].

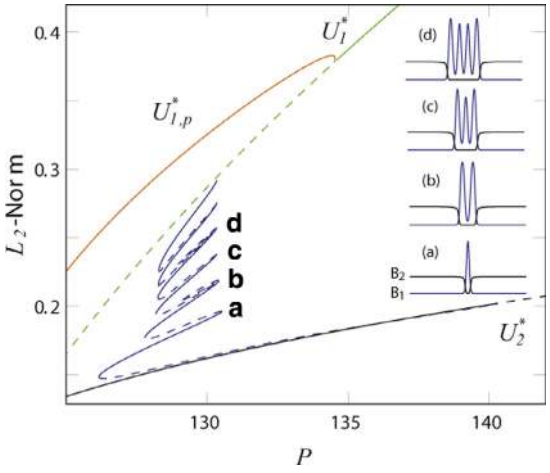

Fig. 17. A bifurcation diagram that includes localized solution branches. The vertical axis is chosen here to be the L_2 norm of the biomass variables ($\|B\| = \int (B_1^2 + B_2^2)^{1/2} dx$). The insets show spatial biomass profiles of hybrid states consisting of confined patterned domains of the $\chi = 0$ functional group (B_1) in uniform distributions of the $\chi = 1$ functional group (B_2). Adapted from [45].

ecosystem function (dotted arrows in Fig. 1). Such links can mediate the relationships between the latter three elements (broken arrows in Fig. 1) as we now discuss.

4.1. Relation between the abiotic environment and ecosystem function

The freedom of spatially extended ecosystems to form patterns opens up new pathways for ecosystem response to changes in the abiotic environment. Responses by pattern formation can affect the nature of desertification transitions, making them gradual rather than abrupt (Section 3.2.1), and can affect the success of restoration practices (Section 3.2.2). These consequences bear, in turn, on ecosystem function in terms of biological productivity and resilience to rainfall variability, as discussed below.

4.1.1. Biological productivity

Two scenarios of gradual desertification have been discussed in Section 3.2.1. The first is associated with a wide band of periodic patterns with increasingly long wavelengths as precipitation drops down. Wide solution bands are typically found in the bistability range of periodic patterns and bare soil, far from the nonuniform instability of uniform vegetation, as Fig. 5 illustrates. Transitions across this band to periodic patterns with longer wavelengths represent a gradual decrease in the total biomass, and thus in the biological productivity, before a transition to bare soil takes place, unlike the direct and sudden collapse to bare soil in the absence of patterns [64].

The second scenario of gradual desertification that has been described is associated with front pinning and homoclinic snaking within a bistability range of uniform and patterned vegetation states. This mechanism applies to landscapes that are initially in a hybrid state or in an initial condition that can converge to a hybrid state in response to a change in the environmental conditions (e.g. a periodic pattern with defects). Gradual desertification in this case can be realized as a cascade of hybrid-state transitions to ever lower biomass states, induced by environmental variability, such as a series of droughts [63,93]. Such cascades have been studied recently using the simplified model Eq. (20) in the bistability range of uniform vegetation and periodic gap patterns [78].

A third scenario of gradual desertification can be realized outside the snaking (or hybrid-state) range, where fronts are not pinned.

This scenario can occur even at constant environmental conditions, unlike the two scenarios discussed above, which require precipitation downshifts. However, even in that case, gradual desertification is a slow process, particularly in large systems, because of the local dynamics it entails.

These results open up new directions for the development of land management practices to mitigate land degradation, that is, practices that favor gradual desertification, which can be easily monitored, over sudden desertification.

4.1.2. Resilience

As Fig. 5 shows, solutions representing periodic vegetation patterns extend to precipitation ranges much lower than the uniform vegetation solution. Thus, the presence of pattern-forming species in a water-limited ecosystem increases the resilience of the ecosystem to droughts. We may further ask whether the pattern type, e.g. spots or stripes, plays a role in the resilience of the ecosystem to environmental variability.

We first address this question in the context of vegetation restoration. In Section 3.2.2 we described the response of an ecosystem to a 1d, stripe-like ground modulations. We showed that restoration in a rhombic pattern, which involves discontinuous plantation along the embankments or the stripes of removed crust, to form a 2d 2:1 resonant pattern (Fig. 11) is more resilient to droughts as compared with continuous plantation to form a 1d 1:1 resonant stripe pattern. This prediction is based on the assumption of weak ground modulations; strong ground modulations may extend the stripe solution branch to lower precipitation and thereby increase their resilience. Weak modulations, however, are advantageous in being more cost effective. Furthermore, although restoration in a rhombic pattern involves partial plantation along the ground modulations (which further reduces the restoration costs), model results show that the total biomass of the restored ecosystem can be as large as in a stripe restoration; the partial area coverage is compensated by a higher biomass areal density because of reduced competition for water.

The relation between pattern type and resilience may also be relevant to the management of functioning ecosystems. Provisioning ecosystem services that involve biomass removal, such as grazing and clear-cutting, may better be conducted in patterns that favor the convergence to a spot pattern rather than to bare soil.

4.2. Relation between the abiotic environment and biodiversity

The significance of environmental heterogeneity to biodiversity has been recognized long ago; one of its earliest expressions is the *habitat heterogeneity hypothesis* according to which an increase in the number of habitats in a landscape reduces species competition by providing more niches and alternative ways of exploiting the environmental resources, and therefore leads to an increase in species diversity [131]. However, the significance of *self-organized* heterogeneity, induced by pattern formation, has hardly been studied. In Section 3.1 we discussed how self-organized heterogeneity of biomass and water changes along the rainfall gradient, and in Section 3.3 we showed that self-organized soil-water heterogeneity, formed by a pattern-forming ecosystem engineer, can affect interspecific interactions. Model studies of these interactions and the implications to biodiversity have been limited so far to simple limiting cases of woody-herbaceous communities: A pattern-forming woody ecosystem engineer interacting with a single herbaceous population (Section 3.3.1), a large non-pattern-forming herbaceous community with no woody species (Section 3.3.2), and a small pattern-forming herbaceous community with no woody species (Section 3.3.2). In the following we project the results of these studies to more complex realizations of woody-herbaceous systems along the rainfall gradient, and relate them to available empirical observations.

4.2.1. A two species woody-herbaceous system

The model results described in Section 3.3.1 show that the interaction between woody and herbaceous life forms can change from competitive (negative) to facilitative (positive) as the precipitation is decreased, and attribute this effect to the ecosystem engineering of the woody life form that develops as the infiltration feedback becomes stronger relative to the root-augmentation feedback. This is consistent with the *stress-gradient hypothesis*, according to which the intensity of facilitation and competition change inversely along environmental gradients with net positive interactions dominating under stressful conditions [132,133]. Indeed, field studies of annual plants in the presence of shrubs have found that at high rainfall the annual biomass was higher in open areas away from shrubs, while at low rainfall, the annual biomass was higher under the shrub canopies [134]. This behavior has been attributed to several factors, some of which are not taken into account by the model, such as higher nutrient concentration under the shrub canopies due to litter decomposition. However, the model studies show that basic aspects of biomass-water interactions at the level of a single patch can already account for the observations by uncovering the roles of two counteracting pattern-forming feedbacks. The expected significance of this patch-scale mechanism is the mitigation of species-diversity decline at low rainfall, because of the mesic habitats that the woody ecosystem engineer forms.

At larger spatial scales additional facilitation mechanisms are predicted; while woody patches in sparse, savanna-like landscapes exclude herbaceous vegetation, patches in dense woody patterns can facilitate its growth. Since different herbaceous species are likely to reside in the open areas and understorey, pattern-dependent ecosystem engineering can be a driver of high species diversity in landscapes that show high pattern diversity [10]. The conditions that lead to pattern diversity are not fully understood at this stage; very few model studies of pattern-forming woody-herbaceous systems have been reported so far [37,135–137] and the full bifurcation diagram for uniform and patterned vegetation states has not been evaluated yet. Nevertheless, a significant result to our context that has been obtained is the existence of a bistability precipitation range of uniform herbaceous vegetation and woody-herbaceous spot patterns [37]. Within this range many hybrid states may exist, including savanna patterns of the type shown in Fig. 13, and additional savanna patterns with larger domains of the spot-pattern state, where herbaceous growth is facilitated understorey (Fig. 13, right panels). The high pattern diversity expected in this bistability range may favor high species diversity [10].

4.2.2. Large non-pattern-forming herbaceous community

In Section 3.3.2 we described the derivation of diversity-precipitation relations for a large herbaceous community, assuming non of the functional groups within the community is pattern forming. The relations show a monotonic increase of diversity with precipitation, in agreement with field studies of annuals in water-limited ecosystems [138]. However, field studies of annuals in the presence of shrubs show a hump-shape relation between the annuals? diversity and precipitation, rather than a monotonic relation [134,139]. The discussion of plants as ecosystem engineers in Section 3.3.1 provides a possible explanation for the observation of a hump shape relation. Patches of shrubs (woody engineer), which facilitate the growth of annuals (herbaceous vegetation) at low precipitation, out compete them at high precipitation, and hardly leave unaffected open areas for the annuals to grow, because of the dense patch patterns they form. As a consequence, a significant decrease in the annuals' diversity is expected at high precipitation. The combined effect is a hump-shaped diversity-precipitation relation, as Fig. 18 illustrates. Hump-shaped relations of this kind can be studied by using Eq. (21) to represent a non-pattern-forming herbaceous community, and

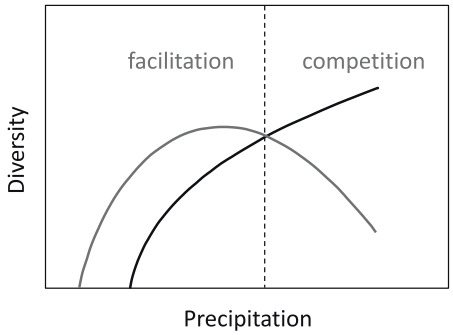

Fig. 18. Schematic illustration of the possible effect of a pattern-forming woody ecosystem engineer on the diversity-precipitation relation of herbaceous plant community. The gray (black) curves show the diversity-precipitation relations in the presence (absence) of a woody engineer. The change from competition and exclusion of herbaceous vegetation at high rainfall to facilitation at low rainfall results in a hump-shape relation.

complementing them with an additional equation for the biomass of a pattern-forming woody engineer.

4.2.3. Small pattern-forming herbaceous community

A different limiting case, also studied in Section 3.3.2, is a small community consisting of two functional groups, one specializing in capturing water ($\chi = 1$) and the other in capturing light ($\chi = 0$). Both functional groups can form spatial patterns but at different precipitation ranges. In particular, a bistability range of two pure-population states can be identified where one functional group is pattern forming and the other is not. Front pinning in this range results in spatial coexistence in the form of stable mosaics of the two states even though locally each group excludes the other.

For a system consisting of two life forms the range of front pinning (snaking range) may be small and insignificant, as Fig. 17 suggests. In a large community, however, many more bistability or multistability ranges of uniform and patterned states may exist. This suggests a succession of front-pinning ranges along the precipitation axis that involve different life forms, and, therefore, significant changes in community structure along the rainfall gradient. A first step in disentangling this complex problem is the consideration of a three-life-form system. It is worth noting in this regard that although front pinning has been studied mostly in the context of bistability of uniform and patterned states it has also been found in cases where the two stable states are spatially patterned [140]. This suggests even wider ranges of front pinning along the rainfall gradient.

4.3. Relation between biodiversity and ecosystem function

The reciprocal relationships between biodiversity and ecosystem function is a subject of active research [11], but the roles pattern formation can play in these relationships are largely overlooked. We focus here on one example, the encroachment of shrubland into grassland, which has been documented in Southern Africa, South America, Australia and Southwestern United States, and may have both negative and positive effects on ecosystem function [141]. This is an example of a front propagation problem in which interspecific interactions at the front zone determine its direction and speed of propagation.

There are two levels at which this problem can be studied using (9), a small community level, consisting of woody and herbaceous life forms ($n = 2$), and a large community level, consisting of a woody life form and a community of herbaceous functional groups distributed along a tradeoff axis ($n \gg 1$). In the equations for a two-life-form system ($n = 2$) the relevant context is the bistability precipitation range of uniform herbaceous vegetation and woody spot patterns (see Section 4.2.1 and Ref. [37]). Since this is a bistability range of uniform and patterned states, three subranges with distinct dynamical behaviors can be distinguished: a woody spot pattern invading uniform herbaceous vegetation, uniform herbaceous vegetation invading a woody spot pattern, and a subrange in which no invasion takes place in which the front that separates the two alternative states is pinned. This is an open problem that calls for numerical and analytical model studies aimed at identifying the parameters (or initial conditions) that affect the direction of front propagation, and the conditions for front pinning. Model modifications to include the effects of temperature, CO_2 level, fires and grazing may be needed [142].

Studies of the large-community problem are harder but can provide predictions about community-level properties, such as the functional-diversity change that the encroachment of shrubland into grassland induces. Such studies may provide a better understanding of the reported positive and negative effects that this encroachment process has on ecosystem function [141].

5. Conclusion

Using the context of dryland landscapes, and a model platform that describes the dynamics of water-limited plant communities, we discussed mechanisms and manners by which pattern formation can affect the relationships between the abiotic environment, biodiversity and ecosystem function. Some of the model results that have been presented here are supported by (or at least consistent with) field observations, such as the sequence of vegetation states along the rainfall gradient, or the ability of woody plant species to act as ecosystem engineers in stressed environments. Some other results are predictions that, as of yet, lack supporting evidence, such as front pinning.

Since ecosystems are inherently nonlinear and spatially extended, pattern formation phenomena should be expected to be observed in other terrestrial ecosystems, and in marine ecosystems too. Indeed, regular spatial patterns have also been observed and modeled in wetland vegetation [143,144], and in mussels beds [145]. In these examples, as in dryland vegetation, pattern formation results from nonuniform instabilities of uniform states in which the growth of spatially structured modes leads to patterned states. However, pattern formation may also result from uniform instabilities that give rise to a multiplicity of stable uniform states, as patterns consisting of spatial domains occupied by different states are possible [12]. A multiplicity of stable states has been found in studies of tidal marshes [146], plankton systems [147,148] and coastal vegetation [149], and is likely to be found in many more marine or marine-related ecosystems. In all these systems environmental variability may induce pattern-formation processes that can affect biodiversity and ecosystem function.

Finally, the relationships between spatial ecology and pattern formation are not uni-directional; not only can spatial ecology benefit from the concepts and tools of pattern formation theory, it can also pose new interesting questions in pattern-formation research, with possible applications to other contexts. One example is the interplay between different pattern-forming feedbacks that induce the same type of instability, e.g. the infiltration and soil-water diffusion feedbacks [53]. Another example is the collapse of stripe patterns to bare-soil, rather than smooth convergence to rhombic patterns, in restored landscapes subjected to environmental fluctuations [124]. Yet another example is the homoclinic snaking found in the model for two extreme functional groups, which, unlike other examples, consists of a single snaking branch of localized structures that involves both even and odd numbers of peaks [45].

Acknowledgment

This paper describes the works of many students and colleagues of mine, including Golan Bel, Erez Gilad, Lev Haim, Jost von Hardenberg, Shai Kinast, Assaf Kletter, Paris Kyriazopoulos, Yair Mau,

Jonathan Nathan, Yagil Osem, Antonello Provenzale, Moshe Shachak, Hezi Yizhaq, and Yuval Zelnik. The support of the Israel Science Foundation (Grants no. 305/13 and 861/09), the US - Israel Binational Science Foundation (Grant No. 2008241), the James S. McDonnell Foundation (Grant no. 220020056) and the Ministry of Science, Technology and Space, is gratefully acknowledged.

References

[1] G.-R. Walther, et al., Ecological responses to recent climate change, Nature 416 (2002) 389–395.
[2] F. Maestre, R. Salguero-Goómez, J. Quero, It is getting hotter in here: determining and projecting the impacts of global environmental change on drylands, Phil. Trans. R. Soc. B 367 (2012) 3062–3075.
[3] N. Grimm et al., The impacts of climate change on ecosystem structure and function, Front Ecol. Environ. 11 (2013) 474–482.
[4] S.E. Sultan, Phenotypic plasticity for plant development, function and life history, Tr. Plant Sci. 5 (2005) 537–542.
[5] E. Weiher, P. Keddy, Assembly rules, null models, and trait dispersion: new questions from old patterns, Oikos 74 (1995) 159–165.
[6] K. Suding, et al., Scaling environmental change through the community-level: a trait-based response-and-effect framework for plants, Glob. Change Biol. 14 (2008) 1125–1140.
[7] C. Valentine, J. d'Herbes, J. Poesen, Soil and water components of banded vegetation patterns, Catena 37 (1999) 1–24.
[8] V. Deblauwe, N. Barbier, P. Couteron, O. Lejeune, J. Bogaert, The global biogeography of semi-arid periodic vegetation patterns, Glob. Ecol. Biogeogr. 17 (2008) 715–723.
[9] M. Rietkerk, J. van de Koppel, Regular pattern formation in real ecosystems, Tr. Ecol. Evol. 23 (3) (2008) 169–175.
[10] E. Meron, Pattern-formation approach to modelling spatially extended ecosystems, Ecol. Model. 234 (2012) 70–82.
[11] M. Loreau, Linking biodiversity and ecosystems: towards a unifying ecological theory, Phil. Trans. R. Soc. B 265 (2010) 49–60.
[12] E. Meron, Nonlinear Physics of Ecosystems, CRC Press, Taylor & Francis Group, 2015.
[13] V. Grimm, S.F. Railsback, Individual-based Modeling and Ecology, Princeton University Press, 2005.
[14] R.B. Hoyle, Pattern Formation: An Introduction to Methods, Cambridge University Press, 2006.
[15] M. Cross, H. Greenside, Pattern Formation and Dynamics in Nonequilibrium Systems, Cambridge University Press, 2009.
[16] J.H. Schenk, S. Espino, C.M. Goedhart, M. Nordenstahl, H.I. Cabrera, C.S. Jones, Hydraulic integration and shrub growth form linked across continental aridity gradients, Proc. Natl. Acad. Sci. 105 (32) (2008) 11248–11253, doi:10.1073/pnas.0804294105.
[17] R. Lefever, O. Lejeune, On the origin of tiger bush, Bull. Math. Biol. 59 (1997) 263–294.
[18] C. Klausmeier, Regular and irregular patterns in semiarid vegetation, Science 284 (1999) 1826–1828.
[19] J. von Hardenberg, E. Meron, M. Shachak, Y. Zarmi, Diversity of vegitation patterns and desertification, Phys. Rev. Lett. 89 (198101) (2001).
[20] N. Shnerb, P. Sarah, H. Lavee, S. Solomon, Reactive glass and vegetation patterns, Phys. Rev. Lett. 90 (2003) 0381011.
[21] R. HilleRisLambers, M. Rietkerk, F. Van den Bosch, H. Prins, H. de Kroon, Vegetation pattern formation in semi-arid grazing systems, Ecology 82 (2001) 50–61.
[22] E. Gilad, J. Von Hardenberg, A. Provenzale, M. Shachak, E. Meron, Ecosystem engineers: From pattern formation to habitat creation, Phys. Rev. Lett. 93 (098105) (2004).
[23] F. Borgogno, P. D'Odorico, F. Laio, L. Ridolfi, Mathematical models of vegetation pattern formation in ecohydrology, Rev. Geophys. 47 (2009) RG1005.
[24] A. Ana I.Borthagaray, M.A. Fuentes, P.A. Marquet, Vegetation pattern formation in a fog-dependent ecosystem, J. Theor. Biol. 265 (2010) 18–26.
[25] N.E. West, Structure and function of microphytic soil crusts in wildland ecosystems of arid to semi-arid regions, Adv. Ecol. Res. 20 (1990) 179–223.
[26] S. Campbell, Origins of Life 335.
[27] E. Verrecchia, A. Yair, G.J. Kidron, K. Verrecchia, Physical properties of the psammophile cryptogamic crust and their consequences to the water regime of sandy softs, north-western negev desert, israel, J Arid Environ. 29 (1995) 427–437.
[28] D.J. Eldridge, E. Zaady, S. M., Infiltration through three contrasting biological soil crusts in patterned landscapes in the negev, israel, J. Stat. Phys. 148 (2012) 723–739.
[29] M. Shachak, G.M. Lovett, Atmospheric deposition to a desert ecosystem and its implication for management, Ecol. Appl. 8 (1998) 455–463.
[30] J. Puigdefbregas, The role of vegetation patterns in structuring runoff and sediment uxes in drylands, Earth Surf. Process. Landf. 30 (2003) 133–147.
[31] I. Stavi, H. Lavee, E.D. Ungar, P. Sarah, Ecogeomorphic feedbacks in semiarid rangelands: A review, Pedosphere 19 (2) (2009) 217–229.
[32] B. Walker, D. Ludwig, C. Holling, R. Peterman, Stability of semi-arid savana grazing systems, J. Ecol. 69 (1981) 473–498.
[33] A.J. Bloom, F.S. Chapin, H.A. Mooney, Resource Limitation in Plants–An Economic Analogy, Annu. Rev. Ecol. Syst. 16 (1985) 363–392.
[34] K.D.M. McConnaughay, J.S. Coleman, Biomass allocation in plants: Ontogeny or optimality? a test along three resource gradients, Ecology 80 (8) (1999) 2581–2593.
[35] G.C. Evans, The Quantitative Analysis of Plant Growth, University of California Press, 1972.
[36] E. Gilad, J. Von Hardenberg, A. Provenzale, M. Shachak, E. Meron, A mathematical model for plants as ecosystem engineers, J. Theor. Biol. 244 (2007) 680.
[37] E. Gilad, M. Shachak, E. Meron, Dynamics and spatial organization of plant communities in water limited systems, Theor. Popul. Biol. 72 (2007) 214–230.
[38] M. Santillana, C. Dawson, A numerical approach to study the properties of solutions of the diffusive wave approximation of the shallow water equations, Comput. Geosci. 14 (2010) 31–53.
[39] M. Rietkerk, M. Boerlijst, F. van Langevelde, R. HilleRisLambers, J. van de Koppel, L. Kumar, H. Prins, A. De Roos, Self-organization of vegetation in arid ecosystems, Am. Nat. 160 (2002) 524–530.
[40] S. Thompson, G. Katul, S.M. McMahon, Role of biomass spread in vegetation pattern formation within arid ecosystems, Water Resour. Res. 44 (2008) W10421.
[41] R. Nathan, H.C. Muller-Landau, Spatial patterns of seed dispersal, their determinants and consequences for recruitment, Tr. Ecol. Evol. 15 (7) (2000) 278–285, doi:10.1016/S0169-5347(00)01874-7.
[42] P.M. Saco, G.R. Willgoose, G.R. Hancock, Eco-geomorphology of banded vegetation patterns in arid and semi-arid regions, Hydrol. Earth Syst. Sci. 11 (6) (2007) 1717–1730.
[43] S.C. Dekker, M. Rietkerk, M.F.P. Bierkens, Coupling microscale vegetation-soil water and macroscale vegetation-precipitation feedbacks in semiarid ecosystems, Glob. Change Biol. 34 (2007) 671–678.
[44] D. Tilman, Resource competition and community structure, Monographs in Population Biology, Princeton University Press, Princeton, New Jersey, USA, 1982.
[45] P. Kyriazopoulos, N. Jonathan, E. Meron, Species coexistence by front pinning, Ecol. Complex. 20 (2014) 271–281.
[46] J. Nathan, Y. Osem, M. Shachak, E. Meron, Linking functional diversity to resource availability and disturbance: a mechanistic approach for water limited plant communities, Submitted to J. Ecology (2015).
[47] B. James M., F. Joe, S. Mark J., S. Jonathan, C. Sarah J., G. Steve J., T. Richard, A plant trait analysis of responses to grazing in a long-term experiment, J. Appl. Ecol. 38 (2) (2001) 253–267.
[48] S. Diaz, I. Noy-Meir, M. Cabido, Can grazing response of herbaceous plants be predicted from simple vegetative traits? J. Appl. Ecol. 38 (3) (2001) 497–508, doi:10.1046/j.1365-2664.2001.00635.x.
[49] Y. Osem, A. Perevolotsky, J. Kigel, Site productivity and plant size explain the response of annual species to grazing exclusion in a mediterranean semi-arid rangeland, J. Ecol. 92 (2) (2004) 297–309.
[50] S.C. Stearns, Trade-offs in life-history evolution, Funct. Ecol. 3 (1989) 259–268.
[51] E. Ben-Hur, O. Fragman-Sapir, R. Hadas, A. Singer, R. Kadmon, Functional trade-offs increase species diversity in experimental plant communities, Ecol. Lett. 15 (11) (2012) 1276–1282.
[52] G.I. Barenblatt, Scaling, Self-Similarity, and Intermediate Asymptotics, Cambridge University Press, 1996.
[53] S. Kinast, Y.R. Zelnik, G. Bel, E. Meron, Interplay between turing mechanisms can increase pattern diversity, Phys. Rev. Lett. 112 (2014) 078701.
[54] V. Guttal, C. Jayaprakash, Self-organization and productivity in semi-arid ecosystems: implications of seasonality in rainfall., J. Theor. Biol. 248 (3) (2007) 490–500, doi:10.1016/j.jtbi.2007.05.020.
[55] A. Kletter, J. Von Hardenberg, E. Meron, A. Provenzale, Patterned vegetation and rainfall intermittency, J. Theo. Biol. 256 (2009) 574–583.
[56] E. Sheffer, H. Yizhaq, E. Gilad, M. Shachak, E. Meron, Mechanisms of vegetation-ring formation in water-limited systems, J. Theor. Biol. 273 (2011) 138–146.
[57] G. Mcgrath, K. Paik, C. Hinz, Microtopography alters self-organized vegetation patterns in water-limited ecosystems, J. Geophys. Res. G: Biogeosci. 117 (2012) 19, doi:10.1029/2011JG001870.
[58] E. Sheffer, J. von Hardenberg, H. Yizhaq, M. Shachak, E. Meron, Emerged or imposed: a theory on the role of physical templates and self-organisation for vegetation patchiness, Ecol. Lett. 16 (2) (2013) 127–139, doi:10.1111/ele.12027.
[59] H. Yizhaq, S. Sela, T. Svoray, S. Assouline, G. Bel, Effects of heterogeneous soil-water diffusivity on vegetation pattern formation, Water Resour. Res. 50 (2014) 5743–5758, doi:10.1002/2014WR015362.
[60] J.A. Bonachela, R.M. Pringle, E. Sheffer, T.C. Coverdale, J.A. Guyton, K.K. Caylor, S.A. Levin, C.E. Tarnita, Termite mounds can increase the robustness of dryland ecosystems to climatic change, Science 347 (6222) (2015) 651–655.
[61] M.D. Cramer, J.J. Midgley, The distribution and spatial patterning of mima-like mounds in south africa suggests genesis through vegetation induced aeolian sediment deposition, J. Arid Environ. 119 (2015) 16–26.
[62] H.A. Dijkstra, Vegetation pattern formation in a semi-arid climate, Int. J. Bifurc. Chaos 21 (12) (2011) 3497–3509.
[63] Y.R. Zelnik, S. Kinast, H. Yizhaq, G. Bel, E. Meron, Regime shifts in models of dryland vegetation, Philos. Trans. R. Soc. A 371 (2013) 20120358.
[64] K. Siteur, E. Siero, M.B. Eppinga, J.D. Rademacher, A. Doelman, M. Rietkerk, Beyond turing: the response of patterned ecosystems to environmental change, Ecol. Complex. 20 (0) (2014) 81–96.
[65] M. Cross, P. Hohenberg, Pattern formation outside equilibrium, Rev. Mod. Phys. 65 (1993) 851.
[66] L. Pismen, Patterns and Interfaces in Dissipative Dynamics, Springer Series in Synergetics, Springer, 2006.
[67] K. Gowda, H. Riecke, M. Silber, Transitions between patterned states in vegetation models for semiarid ecosystems, Phys. Rev. E 89 (2014) 022701.

[68] H. Yizhaq, E. Gilad, E. Meron, Banded vegetation: biological productivity and resilience, Physica A 356 (2005) 139.
[69] J.A. Sherratt, An analysis of vegetation stripe formation in semi-arid landscapes, J. Math. Biol. 51 (2) (2005) 183–197, doi:10.1007/s00285-005-0319-5.
[70] V. Deblauwe, P. Couteron, O. Lejeune, J. Bogaert, N. Barbier, Environmental modulation of self-organized periodic vegetation patterns in sudan, Ecography 33 (2010) 1–13.
[71] J.A. Sherratt, A.D. Synodinos, Vegetation patterns and desertification waves in semi-aridenvironments: mathematical models based on local facilitation in plants, Discret. Contin. Dyn. Syst. Ser. B 17 (2012) 2815–2827.
[72] V. Deblauwe, P. Couteron, J. Bogaert, N. Barbier, Determinants and dynamics of banded vegetation pattern migration in arid climates, Ecol. Monogr. 82 (2012) 3–21.
[73] J.A. Sherratt, Using wavelength and slope to infer the historical origin of semiarid vegetation bands, Proc. Natl. Acad. Sci. 112 (14) (2015) 4202–4207, doi:10.1073/pnas.1420171112.
[74] E. Knobloch, Spatially localized structures in dissipative systems: open problems, Nonlinearity 21 (2008) T45.
[75] E. Knobloch, Spatial localization in dissipative systems, Annu. Rev. Condens. Matter Phys. 6 (1) (2015) 325–359.
[76] Y. Pomeau, Front motion, metastability and subcritical bifurcations in hydrodynamics, Physica D 23 (1986) 3–11.
[77] S. Getzin, K. Wiegand, T. Wiegand, H. Yizhaq, J. von Hardenberg, E. Meron, Adopting a spatially explicit perspective to study the mysterious fairy circles of namibia, Ecography 38 (2015) 1–11.
[78] Y.R. Zelnik, E. Meron, G. Bel, Gradual regime shifts in fairy circles, Proc. Natl. Acad. Sci. 112 (2015) 12327–12331.
[79] J. Carr, R.L. Pego, Metastable patterns in solutions of $ut = 2uxxf(u)$, Communi. Pure Appl. Math. 42 (5) (1989) 523–576.
[80] T.M. Scanlon, K.C. Kelly, S.A. Levin, I. Rodriguez-Iturbe, Positive feedbacks promote power-law clustering of kalahari vegetation, nature 449 (2007) 209–212.
[81] S. Kéfi, M. Rietkerk, C.L. Alados, Y. Pueyo, V.P. Papanastasis, A. ElAich, P.C. de Ruiter, Spatial vegetation patterns and imminent desertification in mediterranean arid ecosystems, nature 449 (2007) 213–216.
[82] A. Manor, N. Shnerb, Facilitation, competition, and vegetation patchiness: From scale free distributions to patterns, J. Theor. Biol. 253 (2011) 838–842.
[83] J. von Hardenberg, A.Y. Kletter, H. Yizhaq, J. Nathan, E. Meron, Periodic vs. scale-free patterns in dryland vegetation, Proc. R. Soc. B 277 (2010) 1771–1776.
[84] E. Sheffer, H. Yizhaq, E. Gilad, M. Shachak, E. Meron, Why do plants in resource deprived environments form rings? Ecol. Complex. 4 (2007) 192–200.
[85] A.Y. Kletter, J. von Hardenberg, E. Meron, Ostwald ripening in dryland vegetation, Commun. Pure Appl. Anal. 11 (2012) 261–273.
[86] B. Meerson, P.V. Sasorov, Domain stability, competition, growth, and selection in globally constrained bistable systems, Phys. Rev. E 53 (1996) 3491–3494.
[87] E. Meron, H. Yizhaq, E. Gilad, Localized structures in dryland vegetation: Forms and functions, Chaos 17 (037109) (2007).
[88] S. Ravi, P. D'Odorico, L. Wang, S. Collins, Form and function of grass ring patterns in arid grasslands: the role of abiotic controls, Oecologia 158 (2008) 545–555.
[89] F. Carten, A. Marasco, G. Bonanomi, S. Mazzoleni, M. Rietkerk, F. Giannino, Negative plant soil feedback explaining ring formation in clonal plants, J. Theor. Biol. 313 (2012) 153–161.
[90] S. Mazzoleni, G. Bonanomi, G. Incerti, M.L. Chiusano, P. Termolino, A. Mingo, M. Senatore, F. Giannino, F. CartenÃň, M. Rietkerk, V. Lanzotti, Inhibitory and toxic effects of extracellular self-dna in litter: a mechanism for negative plantsoil feedbacks? New Phytologist 205 (2015) 1195–1210.
[91] G. Bonanomi, G. Incerti, A. Stinca, F. Carten, F. Giannino, S. Mazzoleni, Ring formation in clonal plants, Community Ecol. 15 (2014) 77–86.
[92] M. Scheffer, S. Carpenter, J.A. Foley, C. Folke, W. B., Catastrophic shifts in ecosystems, Nature 413 (2001) 53–59.
[93] G. Bel, A. Hagberg, E. Meron, Gradual regime shifts in spatially extended ecosystems, Theor. Ecol. 5 (2012) 591–604.
[94] M. Scheffer, J. Bascompte, W.A. Brock, V. Brovkin, S.R. Carpenter, V. Dakos, H. Held, E.H. van Nes, M. Rietkerk, G. Sugihara, Early-warning signals for critical transitions, Nature 461 (2009) 387–393.
[95] I.A. van de Leemput, E.H. van Nes, M. Scheffer, Resilience of alternative states in spatially extended ecosystems, PLoS ONE 10 (2015) e0116859.
[96] A. Hagberg, E. Meron, Pattern formation in non-gradient reaction diffusion systems: the effects of front bifurcations, Nonlinearity 7 (1994) 805–835.
[97] A. Hagberg, E. Meron, From labyrinthine patterns to spiral turbulence, Phys. Rev. Lett. 72 (1994) 2494–2497.
[98] A. Hagberg, E. Meron, Complex patterns in reaction diffusion systems: a tale of two front instabilities, Chaos 4 (1994c) 477–484.
[99] A. Hagberg, E. Meron, The dynamics of curved fronts: Beyond geometry, Phys. Rev. Lett. 78 (1997) 1166–1169.
[100] B. Marts, A. Hagberg, E. Meron, A. Lin, Bloch-front turbulence in a periodically forced belousov-zhabotinsky reaction, Phys. Rev. Lett. 93 (108305) (2004) 1–4.
[101] M. Mimura, M. Tohma, Dynamic coexistence in a three-species competitiondiffusion system, Ecological Complexity 21 (2015) 215–232.
[102] S. van der Stelt, A. Doelman, G.M. Hek, J. Rademacher, Rise and fall of periodic patterns for a generalized klausmeier-gray-scott model, J. Nonlinear Sci. 23 (2013) 39–95.
[103] P. Gandhi, E. Knobloch, C. Beaume, Localized states in periodically forced systems, Phys. Rev. Lett. 114 (2015) 034102.
[104] D. Machiwal, M.K. JHA, P.K. Singh, S.C. Mahnot, A. Gupta, Planning and design of cost-effective water harvesting structures for efficient utilization of scarce water resources in semi-arid regions of Rajasthan, India, Water Resour. Manage. 18 (2004) 219–235.
[105] R.E. Kelly, D. Pal, Thermal convection with spatially periodic boundary conditions resonant wavelength excitation, J. Fluid Mech. 86 (1978) 433–456.
[106] M. Lowe, J.P. Gollub, T.C. Lubensky, Commensurate and incommensurate structures in a nonequilibrium system, Phys. Rev. Lett. 51 (1983) 786–789.
[107] P. Coulet, Commensurate-incommensurate transition in nonequilibrium systems, Phys. Rev. Lett. 56 (1986) 724.
[108] R. Schmitz, W. Zimmermann, Spatially periodic modulated rayleigh bénard convection, Phys. Rev. E 53 (1996) 5993–6011.
[109] M. Henriot, J. Burguete, R. Ribotta, Entrainment of a spatially extended nonlinear structure under selective forcing, Phys. Rev. Lett. 91 (10) (2003) 104501.
[110] R. Peter, M. Hilt, F. Ziebert, J. Bammert, C. Erlenkamper, N. Lorscheid, C. Weitenberg, A. Winter, M. Hammelle, W. Zimmermann, Stripe-hexagon competition in forced pattern-forming systems with broken up-down symmetry, Phys. Rev. E 71 (2005) 046212.
[111] G. Seiden, S. Weiss, J. McCoy, W. Pesch, E. Bodenschatz, Rayleigh bénard convection in the presence of spatial temperature modulations, Phys. Rev. Lett. 101 (2008) 214503.
[112] R. Manor, A. Hagberg, E. Meron, Wavenumber locking in spatially forced pattern-forming systems, Europhys. Lett. 83 (10005) (2008).
[113] R. Manor, A. Hagberg, E. Meron, Wavenumber locking and pattern formation in spatially forced systems, New J. Phys. 11 (063016) (2009).
[114] G. Freund, W. Pesch, W. Zimmermann, Rayleigh bénard convection in the presence of spatial temperature modulations, J. Fluid Mech. 673 (2011) 318–348.
[115] M. Dolnik, T. Bánsági, S. Ansari, I. Valent, I. Epstein, Locking of turing patterns in the chlorine dioxide-iodine-malonic acid reaction with one-dimensional spatial periodic forcing, Phys. Chem. Chem. Phys. 13 (2011) 12578–12583.
[116] Y. Mau, A. Hagberg, E. Meron, Spatial periodic forcing can displace patterns it is intended to control, Phys. Rev. Lett. 109 (2012) 034102.
[117] D. Feldman, R. Nagao, T. Bansagi Jr., I.R. Epstein, M. Dolnik, Turing patterns in the chlorine dioxide-iodine-malonic acid reaction with square spatial periodic forcing, Phys. Chem. Chem. Phys. 14 (2012) 6577–6583.
[118] M.Z. Hossain, J.M. Floryan, Instabilities of natural convection in a periodically heated layer, J. Fluid Mech. 733 (2013) 33–67.
[119] Y. Mau, L. Haim, A. Hagberg, E. Meron, Competing resonances in spatially forced pattern-forming systems, Phys. Rev. E 88 (2013) 032917.
[120] S. Weiss, G. Seiden, E. Bodenschatz, Resonance patterns in spatially forced rayleighbnard convection, J. Fluid Mech. 756 (2014) 293–308.
[121] L. Haim, Y. Mau, E. Meron, Spatial forcing of pattern-forming systems that lack inversion symmetry, Phys. Rev. E 90 (2) (2014) 022904.
[122] L. Haim, A. Hagberg, R. Nagao, A.P. Steinberg, M. Dolnik, I.R. Epstein, E. Meron, Fronts and patterns in a spatially forced cdima reaction, Phys. Chem. Chem. Phys.: PCCP 16 (47) (2014) 26137–26143, doi:10.1039/c4cp04261a.
[123] H.-C. Kao, C. Beaume, E. Knobloch, Spatial localization in heterogeneous systems, Phys. Rev. E 89 (2014) 012903.
[124] Y. Mau, L. Haim, E. Meron, Reversing desertification as a spatial resonance problem, Phys. Rev. E 91 (2015) 012903.
[125] C. Jones, J. Lawton, M. Shachak, Organisms as ecosystem engineers, Oikos 69 (1994) 373–386.
[126] C. Jones, J. Lawton, M. Shachak, Positive and negative effects of organisms as ecosystem engineers, Ecology 78 (1997) 1946–1957.
[127] K. Cuddington, J. Byers, A. Hastings, W. Wilson (Eds.), Ecosystem Engineers: plants to Protists, Academic Press, 2007.
[128] F.I. Pugnaire, M.T. Luque, Changes in plant interactions along a gradient of environmental stress, Oikos 93 (2001) 42–49.
[129] M. Segoli, E.D. Ungar, I. Giladi, A. Arnon, M. Shachak, Untangling the positive and negative effects of shrubs on herbaceous vegetation in drylands, Landsc. Ecol. 27 (2012) 899–910.
[130] J. Norberg, D.P. Swaney, J. Dushoff, J. Lin, R. Casagrandi, S.A. Levin, Phenotypic diversity and ecosystem functioning in changing environments: a theoretical framework, in: Proceedings of the National Academy of Sciences of the United States of America 98(20) 11376–11381.
[131] J. Tews, U. Brose, V. Grimm, K. Tielbörger, M.C. Wichmann, M. Schwager, F. Jeltsch, Animal species diversity driven by habitat heterogeneity/diversity: the importance of keystone structures, J. Biogeogr. 31 (2004) 79–92.
[132] R.W. Brooker, F.T. Maestre, R.M. Callaway, C.L. Lortie, L.A. Cavieres, G. Kunstler, P. Liancourt, K. Tielbrger, J.M.J. Travis, F. Anthelme, C. Armas, L. Coll, E. Corcket, S. Delzon, E. Forey, Z. Kikvidze, J. Olofsson, F. Pugnaire, C.L. Quiroz, P. Saccone, K. Schiffers, M. Seifan, B. Touzard, R. Michalet, Facilitation in plant communities: the past, the present, and the future, J. Ecol. 96 (1) (2008) 18–34.
[133] D. Malkinson, K. Tielbörger, What does the stress-gradient hypothesis predict? resolving the discrepancies, Oikos 119 (10) (2010) 1546–1552.
[134] C. Holzapfel, K. Tielbörger, H.A. Parag, J. Kigel, S. M., Annual plant-shrub interactions along an aridity gradient, Basic Appl. Ecol. 7 (2006) 268–279.
[135] P. D'Odorico, F. Laio, A. Porporato, L. Ridolfi, N. Barbier, Noise-induced vegetation patterns in fire-prone savannas, J. Geophys. Res.: Biogeosci. 112 (G2) (2007) G02021.
[136] J. Nathan, J. von Hardenberg, E. Meron, Spatial instabilities untie the exclusion-principle constraint on species coexistence, J. Theor. Biol. 335 (2013) 198–204.
[137] M. Baudena, M. Rietkerk, Complexity and coexistence in a simple spatial model for arid savanna ecosystems, Theor. Ecol. 6 (2) (2013) 131–141, doi:10.1007/s12080-012-0165-1.

[138] Y. Osem, A. Perevolotsky, J. Kigel, Grazing effect on diversity of annual plant communities in a semi-arid rangeland: interactions with small-scale spatial and temporal variation in primary productivity, J. Ecol. 90 (6) (2002) 936–946.
[139] R. Michalet, R.W. Brooker, L.A. Cavieres, Z. Kikvidze, C.J. Lortie, F.I. Pugnaire, A. Valiente-Banuet, R.M. Callaway, Do biotic interactions shape both sides of the humped-back model of species richness in plant communities? Ecol. Lett. 9 (7) (2006) 767–773.
[140] H. Uecker, D. Wetzel, Numerical results for snaking of patterns over patterns in some 2d Selkov–Schnakenberg reaction-diffusion systems, SIAM J. Appl. Dyn. Syst. 13 (1) (2014) 94–128.
[141] D.J. Eldridge, M.A. Bowker, F.T. Maestre, E. Roger, R.J. F., W.W. G., Impacts of shrub encroachment on ecosystem structure and functioning: towards a global synthesis, Ecol. Lett. 14 (2011) 709–722.
[142] P. D'Odorico, G.S. Okin, B.T. Bestelmeyer, A synthetic review of feedbacks and drivers of shrub encroachment in arid grasslands, Ecohydrology 5 (5) (2012) 520–530.
[143] M.B. Eppinga, M. Rietkerk, M.J. Wassen, P.C. De Ruiter, Linking habitat modification to catastrophic shifts and vegetation patterns in bogs, Plant Ecol. 200 (2009) 53–68.
[144] Y. Cheng, M. Stieglitz, G. Turk, V. Engel, Effects of anisotropy on pattern formation in wetland ecosystems, Geophys. Res. Lett. 38 (4) (2011) L04402.
[145] Q.-X. Liu, A. Doelman, V. Rottschfer, M. de Jager, P.M.J. Herman, M. Rietkerk, J. van de Koppel, Phase separation explains a new class of self-organized spatial patterns in ecological systems, Proc. Natl. Acad. Sci. (2013).
[146] M. Marani, C. Da Lio, A. DAlpaos, Vegetation engineers marsh morphology through multiple competing stable states, Proc. Natl. Acad. Sci. 110 (9) (2013) 3259–3263.
[147] A.B. Ryabov, L. R., B. B., Vertical distribution and composition of phytoplankton under the influence of an upper mixed layer, J. Theor. Biol. 263 (1) (2010) 120–133, doi:10.1016/j.jtbi.2009.10.034.
[148] A.B. Ryabov, B. Bernd, A graphical theory of competition on spatial resource gradients, Ecol. Lett. 14 (2011) 220–228.
[149] J. Jiang, G. Daozhou, D.L. DeAngelis, Towards a theory of ecotone resilience: Coastal vegetation on a salinity gradient, Theor. Popul. Biol. 82 (2012) 29–37.